Lappeenranta
University of Technology

Ahti Karjalainen

ONLINE ULTRASOUND MEASUREMENTS OF MEMBRANE COMPACTION

Thesis for the degree of Doctor of Science (Technology) to be presented with due permission for public examination and criticism in the Auditorium 1383 at Lappeenranta University of Technology, Lappeenranta, Finland on the 17th of December, 2010, at noon.

Acta Universitatis
Lappeenrantaensis 409

Supervisor Professor Tuure Tuuva
Department of Technomathematics and Technical Physics
Faculty of Technology
Lappeenranta University of Technology
Finland

Reviewers Adj. Professor Pekka Meriläinen
GE Healthcare
Finland

D.Sc. Eija Tuominen
Helsinki Institute of Physics
Finland

Opponent Adj. Professor Pekka Meriläinen
GE Healthcare
Finland

ISBN 978-952-265-007-8
ISBN 978-952-265-008-5 (PDF)
ISSN 1456-4491
Lappeenrannan teknillinen yliopisto
Digipaino 2010

Abstract

Ahti Karjalainen
Online Ultrasound Measurements of Membrane Compaction
Lappeenranta 2010
75 pages
Acta Universitatis Lappeenrantaensis 409
Diss. Lappeenranta University of Technology
ISBN 978-952-265-007-8, ISBN 978-952-265-008-5 (PDF), ISSN 1456-4491

There are several filtration applications in the pulp and paper industry where the capacity and cost-effectiveness of processes are of importance. Ultrafiltration is used to clean process water. Ultrafiltration is a membrane process that separates a certain component or compound from a liquid stream. The pressure difference across the membrane sieves macromolecules smaller than 0.001-0.02 µm through the membrane.

When optimizing the filtration process capacity, online information about the conditions of the membrane is needed. Fouling and compaction of the membrane both affect the capacity of the filtration process. In fouling a "cake" layer starts to build on the surface of the membrane. This layer blocks the molecules from sieving through the membrane thereby decreasing the yield of the process.

In compaction of the membrane the structure is flattened out because of the high pressure applied. The higher pressure increases the capacity but may damage the structure of the membrane permanently. Information about the compaction is needed to effectively operate the filters.

The objective of this study was to develop an accurate system for online monitoring of the condition of the membrane using ultrasound reflectometry. Measurements of ultrafiltration membrane compaction were made successfully utilizing ultrasound. The results were confirmed by permeate flux decline, measurements of compaction with a micrometer, mechanical compaction using a hydraulic piston and a scanning electron microscope (SEM).

The scientific contribution of this thesis is to introduce a secondary ultrasound transducer to determine the speed of sound in the fluid used. The speed of sound is highly dependent on the temperature and pressure used in the filters. When the exact speed of sound is obtained by the reference transducer, the effect of temperature and pressure is eliminated. This speed is then used to calculate the distances with a higher accuracy. As the accuracy or the resolution of the ultrasound measurement is increased, the method can be applied to a higher amount of applications especially for processes where fouling layers are thinner because of smaller macromolecules.

With the help of the transducer, membrane compaction of 13 µm was measured in the pressure of 5 bars. The results were verified with the permeate flux decline, which indicated that compaction had taken place. The measurements of compaction with a

micrometer showed compaction of 23–26 µm. The results are in the same range and confirm the compaction. Mechanical compaction measurements were made using a hydraulic piston, and the result was the same 13 µm as obtained by applying the ultrasound time domain reflectometry (UTDR). A scanning electron microscope (SEM) was used to study the structure of the samples before and after the compaction.

Keywords: ultrasound, UTDR, compaction, membrane
UDC: 534.321.9 : 66.067.1

Acknowledgements

The work was carried out at the Department of Technomathematics and Technical Physics at Lappeenranta University of Technology, Finland, between 2008 and 2010.

I am indebted to my supervisor Professor Tuure Tuuva for his advice and encouragement during the study. He has been my mentor through out my academic career in ups and downs. I am also grateful to Professor Mika Mänttäri and D.Sc. Mari Kallioinen from the Department of Chemical Technology for the valuable collaboration between departments. From the group of Professor Mänttäri, I would like to thank M.Sc. Hanna Laasonen for taking part in the measurement setup development and doing the morning shifts in the laboratory measurements.

I thank the reviewers, D.Sc. Eija Tuominen and Adjunct Professor Pekka Meriläinen, for their valuable comments and corrections, which significantly helped me to improve the thesis.

I express my warm gratitude to all people who have worked with me during this study. Especially I would like to thank D.Sc. Antti Kosonen for the conversations during lunch and coffee breaks, M.Sc. Markku Jokinen for making the coffee and for the debates about research and topics beyond. Further, my thanks go to M.Sc. Vesa Väisänen for discussions and co-operation in the previous projects. In addition, I am' grateful to my friends outside the university for their support.

I would like to address my gratitude to the financing bodies of this study. Without the founding by the Academy of Finland since 2008, this study would not have been made. I express my thanks to Walter Ahlström Foundation for their long-time acknowledgement and support of my studies. Furthermore, thanks are reserved to Ulla Tuominen Foundation for the support and acknowledgement of my research.

I express my warmest gratitude to my parents Seppo and Riitta for their support and encouragement through out my studies in Lappeenranta. Finally, I owe my thanks to my beloved wife Annukka who has been there for me supporting, encouraging and taking a good care of our lovely daughter Elsa at home, during the long hours spent in the university.

Ahti Karjalainen
December 2010
Lappeenranta, Finland

To Elsa

My daughter, my sunshine.

Contents

Nomenclature

Latin alphabet

A	area	m^2
d	diameter	m
f	frequency	Hz
l	length	m
p	pressure	Pa
T	temperature	^oC
s	distance	m
t	time	s
v	velocity magnitude	m/s
$\mathbf{v}$	velocity vector	m/s
x	x-coordinate	m
y	y-coordinate	m
z	z-coordinate	m
Z	acoustic impedance	Ns/m^3

Greek alphabet

Δ	change in the value	
ρ	density	kg/m^3
ω	angular speed	1/s

Subscripts

i	incident
r	reflected
t	transmitted
1	medium 1
2	medium 2

Abbreviations

AC	Alternating current
BNC	Bayonet Neill-Concelman
NDT	non-destructive testing
PCB	printed circuit board
PET	Polyethylene terephthalate

PP	polypropylene
PVDF	Polyvinylidene fluoride
PZT	Lead Zirconate Titanate
RO	Reverse Osmosis
SEI	Secondary electron imaging
SEM	scanning electron microscope
SMA	sub miniature version A
UTDR	ultrasound time domain reflectometry

1 Introduction

This study has been carried out at Lappeenranta University of Technology in collaboration with the Laboratory of Technical Physics and the Laboratory of Membrane Technology. There are several filtration applications in the pulp and paper industry where the capacity and cost-effectiveness of the processes are highly important. Ultrafiltration is used to clean process water. Ultrafiltration is a membrane process that separates a certain component or compound from a liquid stream. The pressure difference across the membrane sieves macromolecules smaller than 0.001–0.02 µm through the membrane (Kallioinen 2/2007).

1.1 Background and motivation

When optimizing the filtration process capacity, online information about the conditions of the membrane is needed. Fouling and compaction of the membrane both affect the capacity of the filtration process. In fouling, "cake" layer starts to build on the surface of the membrane. This layer blocks the molecules from sieving through the membrane thereby decreasing the yield of the process.

In compaction of the membrane the structure is flattened out because of the high pressure applied. The higher pressure increases the capacity but may damage the structure of the membrane permanently. Information about the compaction is needed to effectively operate the filters. To efficiently control the membrane, a method which is based on Non-Destructive Testing (NDT) needs to be used.

There are several different methods to monitor membranes. A review of the methods was given in (Chen V. 2004, Chen J.C. 2004). In the review the methods were divided into optical and non-optical methods. Ultrasound Time Domain Reflectometry (UTDR) was chosen because of its non-invasive nature and low complexity of experiment still achieving good resolution and real–time information. It was also stated that UTDR is one of the few non-invasive methods that could be applied to commercial-scale modules. UTDR uses reflections of the ultrasound to measure distances.

A method applying UTDR in real–time measurement of membrane compaction was presented in (Peterson 1998). It was one of the first publications presenting the use of the UTDR in membrane compaction. Compaction was measured successfully, but rather optimistic value, for the accuracy of the system was assumed to be ±0.75 µm. The error was based on an assumption of the accuracy of the time measurement and it was not measured. A method applying ultrasound on the compaction for gas separation membranes was presented in (Reinsch 2000). The measurements suffered from the temperature affecting the speed of sound and a 1 ºC change in temperature produced an error of 7 µm in the compaction results. More accurate temperature control was

assumed to solve the problem. A method applying UTDR was used to study the effect of filler concentration of the membrane to the membrane compaction in (Aerts 2001).

Mairal from the Greenberg's group also studied real–time measurement of inorganic fouling of reverse osmosis (RO) desalination membranes using ultrasonic time-domain reflectometry in (Mairal 1999 and Mairal 2000). The method used was similar to that presented in (Reinsch 2000); they reported that the growth of the fouling layer was not sufficient enough to produce reflections from the fouling layer. It seemed that the resolution of the system was not adequate enough, so they had to study the amplitude of the reflection. It was shown that the amplitude of the reflection from the membrane surface declined as fouling occurred, and the results were backed up with the permeate flux decline. Although promising results were obtained, further investigation was needed.

Non–invasive monitoring of fouling in a hollow fiber membrane using the UTDR was presented in (Xu 1/2009). Fouling layers were detected successfully, and a scanning electron microscope (SEM) was used to study the fouling layers. The fouling layers formed were quite thick, and they occurred already after an hour of filtration. The resolution of system was not mentioned, but the temperature variation was in the range of ± 1 ºC; consequently, because of the temperature changes, it seemed necessary to study thicker layers. Oily waste water was further studied in (Xu 2/2009).

Method based on UTDR was used for visualization of fouling in microfiltration and ultrafiltration membranes in (Li 1/2002, Li 2/2002 and Li 3/2002) Detected layers were approximately 80 µm thick. Ultrasound was used successfully in monitoring the fouling of membranes before and after cleaning process of the filters in (Li 4/2002 and Li2003). Protein fouling of tubular ultrafiltration membranes was studied in (Li2006) but the thickness of the fouling layer was not achieved and there behaviour of amplitude was examined.

1.2 Objective

The objective of this study was to develop an accurate system for monitoring the condition of a membrane using ultrasound reflectometry. In the study the knowledge of the membrane filters in the Laboratory of Membrane Technology and the knowledge of the ultrasound measurements in the Laboratory of Technical Physics was combined. The system was planned to be developed and implemented on filter equipment operating in the dead–end mode. In this type of filter the feed flow is towards the membrane. Measurements of ultrafiltration membrane compaction were to be made applying UTDR. The results were to be confirmed by permeate flux decline, measurements of compaction with a micrometer, mechanical compaction using a hydraulic piston and a scanning electron microscope (SEM).

1.3 Authors contribution

In the field of chemistry, one application for ultrasound measurements has been the monitoring of membrane filter conditions such as compaction and fouling as described in Section 1.1. The accuracy of the methods before has suffered from temperature and pressure changes and the accuracy has been at the level of tens of microns.

The scientific contribution of this thesis is a developed secondary ultrasound transducer to determine the speed of sound in the fluid used. The speed of sound is highly dependent on the temperature and pressure used in the filters.

When the exact speed of sound is obtained by the reference transducer, the effect of temperature and pressure is eliminated. This speed is then used to calculate the distances with a higher accuracy. The accuracy achieved using the reference transducer was less than one micron, which is factor of ten better than reported in the earlier research before. As the accuracy or the resolution of the ultrasound measurement is increased, the method can be applied to a higher number of applications especially in processes where fouling layers are thinner because of smaller macromolecules.

Author has done all the development work described in this thesis. SEM measurements were carried out at the Department of Chemistry and the hydraulic piston measurement of compaction carried out at the Department of Mechanical Engineering.

1.4 Outline of the thesis

This thesis is divided into six chapters. The first chapter, introduction describes the background of the UTDR and the motivation arising from the paper and pulp industry to develop monitoring methods for membrane filters. The objective is to increase the accuracy of the UTDR; to this end, the contribution of the thesis is the reference transducer developed to eliminate temperature and pressure effects. The accuracy achieved using the reference transducer was less than on micron, which is factor of ten better than reported in the earlier research

Chapter 2 focuses on ultrasound propagation in a medium. This chapter describes how ultrasound travels in the medium and how it is reflected. The temperature and pressure changes affecting the speed of sound are explained. Transmission of sound through the two media is explained and important equations are given.

Chapter 3 explains the experimental part of the thesis by presenting the measurement setup used and the transducers developed to improve the accuracy of the ultrasound

monitoring system. The parts in the setup are explained, and it is described how they work together with the transducers to measure the distance to the membrane.

Chapter 4 introduces the results for the measured accuracy of the system and compaction of the membrane using ultrasound. Because of improved accuracy the system is able to detect compaction of 13 µm. Permeate flux decline is combined to the compaction of the membrane to back up the results obtained. The micrometer measurements also show that the compaction of membrane has occurred. Mechanical measurements of the compaction were carried out using a hydraulic piston. The results are convergent with the results obtained using ultrasound. A scanning electron microscope analysis is presented in the results to study the change in the structure after the compaction.

Chapter 5 analyzes the results obtained using ultrasound and show them to be reliable based on the permeate flux decline and compaction measurements performed with a micrometer, a hydraulic piston and an SEM analysis.

Chapter 6 provides conclusions summing up the results and suggesting some objectives for further work. The system was used to monitor membrane conditions online without affecting the filtering process. Transducers were developed for ultrasound measurements, and a reference transducer was used successfully to improve the resolution of the measurement.

2 Ultrasound propagation in a medium

Ultrasound is defined as the cyclic sound pressure with a frequency of higher than the upper limit of human ear recognition. Depending on the person the upper limit is in the region of 20 kHz. Usually, non-destructive testing (NDT) solutions use frequencies in the range of 1–100 MHz or higher. With a higher frequency, the resolution is better but the disadvantage is that the attenuation in the medium increases.

There are two basic ultrasound measurements methods, namely pulse-echo and transmission through. In the transmission through there are two ultrasound probes, one transmitting and the other receiving, and the material examined is placed between these probes. In the pulse-echo method, the same probe is used in transmitting and receiving of ultrasound signals.

In both of these methods, the transducers consist of a piezoelectric material, which starts to oscillate when a short–pulsed voltage is applied across it. Pulse-echo mode oscillation travels through the medium, and it is reflected when reaching the border of different medium. The reflected wave is then received by the same transducer, and oscillation is again transformed into voltage across the piezoelectric material.

An oscilloscope is used to measure the voltage and time information of both the short time pulsed voltage that starts the oscillation in the piezoelectric material and the reflected wave from the border of media. In Figure 2.1 on the left there is the transmitted pulse and on the right the received reflected wave pulse.

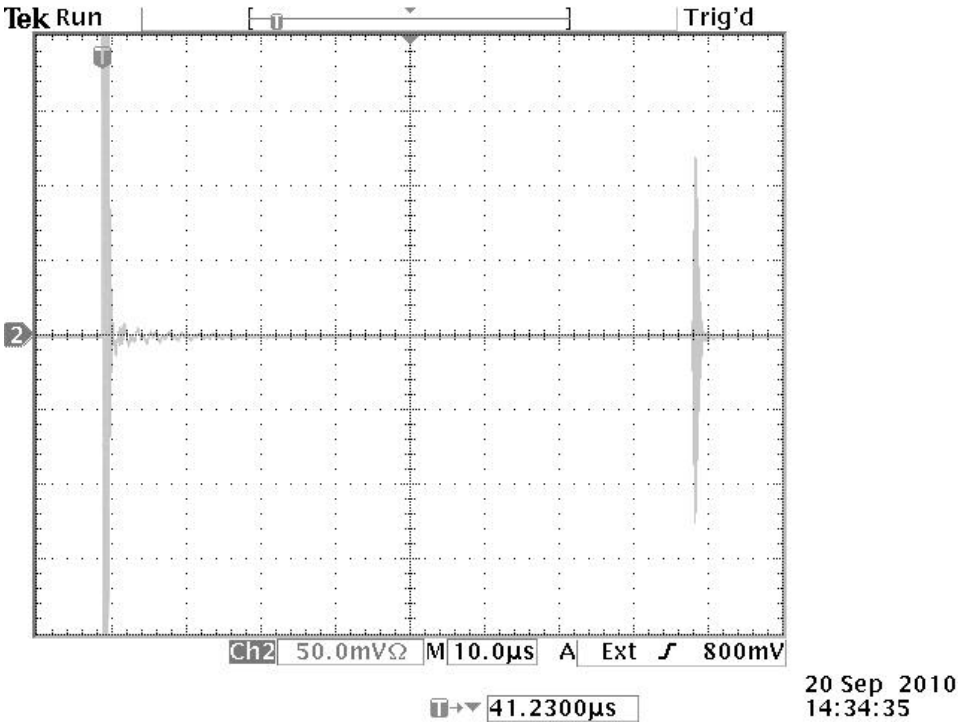

Figure 2.1: Oscilloscope image of a pulse-echo measurement: the transmitted pulse on the left and the received reflected pulse on the right. Half of the time difference of the pulses multiplied by the speed of sound in the medium is now the distance between the transducer and the reflection.

The speed of sound in the medium is known constant. The distance between the transducer and the reflection is.

$$s = \frac{1}{2} \mathrm{v} \Delta t \tag{2.1}$$

Where v is the speed of sound in a medium and Δt the time between the transmitted pulse and the received echo pulse. The time monitored as seen in Figure 2.1 actually corresponds to double the distance to be measured, and thus divided by two.

2.1 Temperature and pressure influence on the speed of sound

The speed of sound in a medium is typically assumed constant. This applies only when the temperature and pressure are not changing. Belogol'skii, Sekoyan et al. made measurements for the speed of sound in pure water (Belogol'skii 1999) using the equation for the speed of sound in atmospheric pressure by (Bilaniuk 1993).

$$c(T,P) = c(T,0) + M_1(T)(P - 0.101325) + M_2(T)(P - 0.101325)^2 + M_3(T)(P - 0.101325)^3 \quad (2.2)$$

where

$$c(T,0) = a_{00} + a_{10}T + a_{20}T^2 + a_{30}T^3 + a_{40}T^4 + a_{50}T^5 \quad (2.3)$$

$$M_1(T) = a_{01} + a_{11}T + a_{21}T^2 + a_{31}T^3 \quad (2.4)$$

$$M_2(T) = a_{02} + a_{12}T + a_{22}T^2 + a_{32}T^3 \quad (2.5)$$

$$M_3(T) = a_{03} + a_{13}T + a_{23}T^2 + a_{33}T^3 \quad (2.6)$$

In the equations above T is the temperature in degrees Celsius and P is the pressure in MPa. The validity of the equations is in the ranges of temperature 0-40 ºC and pressure 0.1–60 MPa, respectively. A table of coefficients for Equations (2.2)–(2.6) is presented in Appendix A.

To show the effect of temperature on the speed of sound, values near the temperature of the actual filtration process were chosen. Using a temperature range of 20–30 ºC and a pressure of 1 bar, the speed of sound in pure water was calculated using the Belogol'skii equations (2.2)–(2.6). The speed of sound as a function of temperature is presented in Figure 2.2.

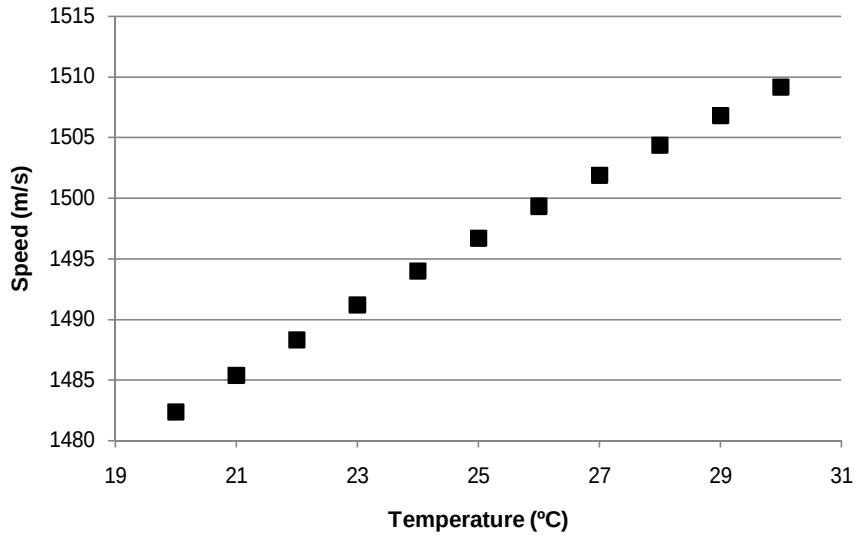

Figure 2.2: Speed of sound in pure water as a function of temperature in 1 bar using the Belogol'skii equations (2.2)–(2.6).

As shown in Figure 2.2, the speed of sound increases rapidly if the temperature rises. This effect must be considered when ultrasound measurements are made and water is the medium.

The effect of pressure on the speed of sound values has also to be taken into account. An actual filtration pressure range of 1–5 bars was chosen and the speed of sound in pure water at a temperature of 25 ºC was plotted in Figure 2.3, using the Belogol'skii equations (2.2)–(2.6).

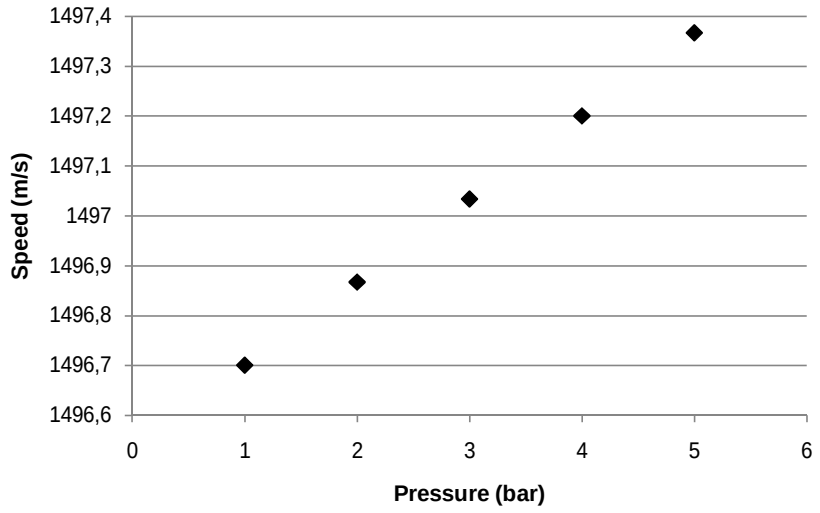

Figure 2.3: Speed of sound in pure water as a function of pressure in 25 ºC using the Belogol'skii equations (2.2)-(2.6).

A higher pressure increases the speed of sound in water but not as strongly as the temperature. The influence of pressure should also be taken into account when performing measurements that require high accuracy.

2.2 Transmission of sound through two media

In a normal incidence, a propagating plane wave meets a smooth surface separating the media 1 and 2 at angle of 90º as shown in Figure 2.4. The reflected and transmitted waves do not refract from the direction of the incident wave. This means that there will be only one possible transmitted and one reflected wave.

To determine how much of the incident wave is transmitted and how much is reflected the, first boundary condition is the continuity of the particle velocity. Particle velocity is velocity of particle in a medium as it transmits a wave. The sum of particle velocities at the boundary in medium 1 equals those in medium2:

$$\underline{v}_{\text{particle}_i} + \underline{v}_{\text{particle}_r} = \underline{v}_{\text{particle}_t} \tag{2.7}$$

where $\underline{v}_{\text{particle}} = \underline{V}e^{j(\omega t - \underline{k}\cdot\underline{r})} = \partial\underline{u}/\partial t, \underline{V}$ is the amplitude coefficient and the subscripts *i*, *r* and *t* refer to the incident, reflected and transmitted waves, respectively.

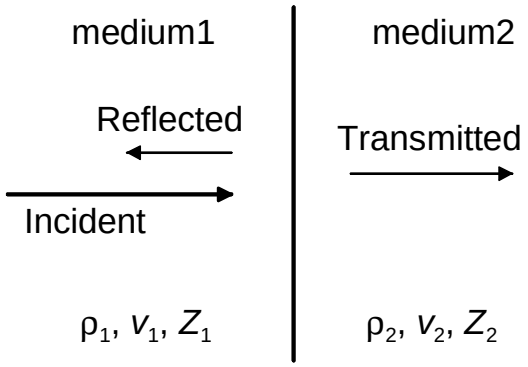

Figure 2.4: Reflection and transmission of a normal incident wave at a boundary of media

Particle velocity of each wave is confined to *phase* propagation in the *x*-direction $\left(\vec{k} \cdot \vec{r} = k_x x\right)$. Thus

$$V_i e^{j(\omega_1 t - k_1 x)} + V_r e^{j(\omega_1 t - k_1 x)} = V_t e^{j(\omega_2 t - k_2 x)} \tag{2.8}$$

Knowing that the acoustic pressure varies as $p = Pe^{j\left(\omega t - \vec{k} \cdot \vec{r}\right)}$, the second boundary condition, the continuity of the acoustic pressure (stress), can be written as

$$P_i e^{j(\omega_1 t - k_1 x)} + P_r e^{j(\omega_1 t - k_1 x)} = P_t e^{j(\omega_2 t - k_2 x)} \tag{2.9}$$

Because the boundary is placed at $x = 0$ and the wave is propagating in the *x*-direction, $\vec{k} \cdot \vec{r} = k_x x = 0$. Assume the continuity of the frequency across the boundary $\omega_1 = \omega_2$. At the boundary, Equations (2.8) and (2.9) can be written as

$$V_i + V_r = V_t \tag{2.10}$$

and

$$P_i + P_r = P_t \tag{2.11}$$

The reflection coefficient is defined as

$$r = \frac{P_r}{P_i} \tag{2.12}$$

and the transmission coefficient as

$$t = \frac{P_t}{P_i} \tag{2.13}$$

These equations yield the pressure amplitudes of the reflected or transmitted wave. The reflection and transmission of the incident wave are governed by the difference of the acoustic impedances, Z_1 and Z_2. $Z = \rho v$, and it can be calculated from tabulated values of density and velocity, it is known for an acoustic wave:

$$Z = \frac{p}{v_{\text{particle}}} \tag{2.14}$$

where the driving potential p is the instantaneous acoustic pressure on the particles within the medium, v_{particle} is the instantaneous velocity of the oscillating particles and Z is the impedance to the movement of the particles within the medium. Using Equation 2.14, the acoustic impedance in materials 1 and 2 is

$$Z_1 = \frac{p_i}{v_{\text{particle}_i}} = \frac{P_i}{V_i} \tag{2.15}$$

$$Z_1 = \frac{p_r}{v_{\text{particle}_r}} = \frac{P_r}{V_r} \tag{2.16}$$

and

$$Z_2 = \frac{p_t}{v_{\text{particle}_t}} \text{ or } Z_2 = \frac{p_i + p_r}{v_{\text{particle}_i} + v_{\text{particle}_r}} = \frac{P_i + P_r}{V_i + V_r} \tag{2.17}$$

Substituting Equations 2.15–2.17 in Equation 2.10 and bearing in mind that the positive direction of the speed is in the incident wave direction, the reflection and transmission coefficients can be written in terms of acoustic impedances:

$$r = \frac{Z_2 - Z_1}{Z_2 + Z_1} \tag{2.18}$$

and

$$t = \frac{2Z_2}{Z_2 + Z_1} \tag{2.19}$$

These amplitude ratios for pressure are called the acoustic Fresnel equations for an isotropic, homogenous medium with a wave at a normal incidence. (Shull 2002)

3 Methods

The experimental procedures applied to implement the reference transducer increasing the accuracy of the distance measurement in this thesis are summarised in the following chapters. The ultrasound measurements of the membrane samples were carried out by using small membrane filter equipment operating in the dead–end mode. In this filter, the feed and concentrate were on the top and the filtered permeate on the bottom. The pressure difference across the membrane was obtained by using an rpm-controlled pump and a mechanical valve in the concentrate flow. The polypropylene (PP) material was used in the filter cylinder and piston. The system was designed so that the maximum pressure limit was over 6 bar. The maximum pressure used in the measurements was 5 bar.

Ion–exchanged water was used in the fluid circulation of the system, this meant that the medium was water also in the ultrasound measurements. The temperature of the water was measured in both the feed water tank and inside the filter. The temperature of the system was kept close to 25 ºC, which is the temperature used in many filter solutions. To prevent a temperature rise because of the pump warming and a higher pressure, ice was added to the feed water tank.

3.1 Setup

The ultrasound measurement setup consists of two parts, the electronic part and the water circulation part (Figure 3.1). The electronic part consists of a pulser which generates short–time voltage pulses that make the transducers vibrate at their resonance frequency. The pulser is connected a with sync wire to an oscilloscope, which is triggered when a pulser signal is applied. Synchronisation between the pulser and the oscilloscope is achieved, and time information is accurate between these instruments.

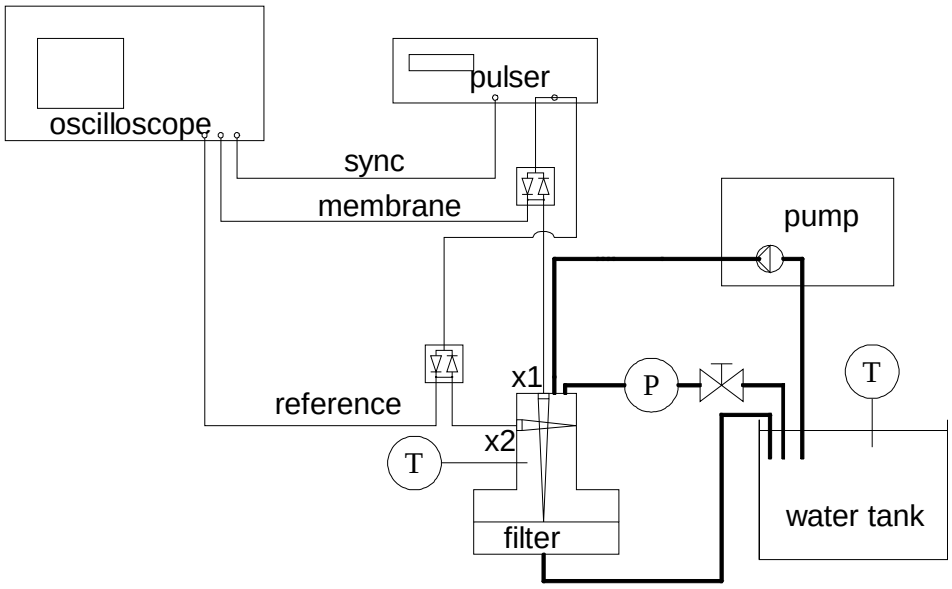

Figure 3.1: Block diagram of the ultrasound measurement setup. Electric wires are illustrated with thin lines and water circulation tubes with thick lines. Reference transducer x2 inside the filter measuring a fixed distance horizontally and the membrane transducer x1 measuring the distance to the membrane.

Transducer vibrations are then transmitted into water and reflected from the surface of the membrane. The reflected pulse is again transformed from acoustic pressure to voltage in the transducer. This voltage is then seen on the oscilloscope as a voltage spike after the pulser voltage. The distance between the transducer and the membrane is described in Equation (2.1). The diode circuit is used to separate the pulser from the oscilloscope and the transducers.

The water circulation part consists of the pump feeding water from the tank into the filter. The filter was pressurized by controlling the speed of the rotation in the pump and the concentrate flux with a mechanical valve. The pressure in the filter was measured from the concentrate flux. The permeate flux refers here to the water that was filtered through the membrane and was returned to the water tank.

The ultrasound measurement setup is illustrated in Figure 3.2. All the instruments are placed as in the block diagram of the setup (Figure 3.1). Transducer reflections can be seen on the oscilloscope screen. The scale, bowl and the stopwatch on left are used to measure the permeate flux.

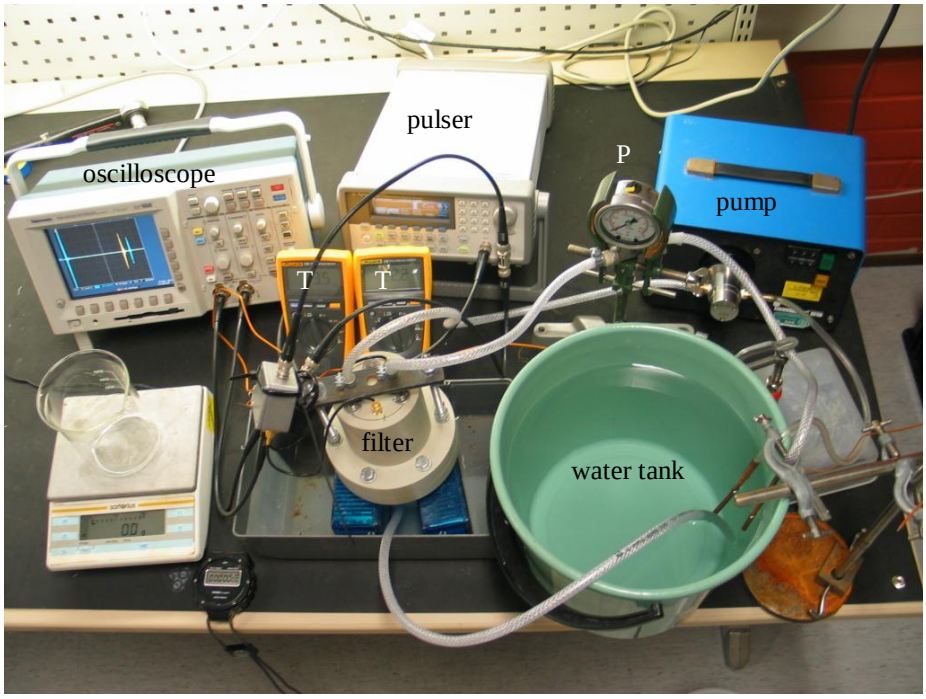

Figure 3.2: Photo of the ultrasound measurement setup. Arrangement of the instruments is the same as in Figure 3.1.

3.2 Transducers

The transducers used in the measurements were designed and built at the Lappeenranta University of Technology. The objective was to develop transducers and not to use industrial ones. Moreover, the transducers were implemented inside the filter, and hence the use of industrial ones would have been difficult.

These transducers are based on a piezoelectric material, which generates a charge when put under a pressure, and will show a change in the volume when an electric field is applied. Piezoelectric materials can be used to transform electrical energy into mechanical energy and vice versa. Furthermore, applying an AC voltage to the material will cause it to vibrate and generate mechanical waves at the same frequency as the electrical voltage. Similarly, if a mechanical vibration is applied, a charge of proportional size and same frequency will be generated (Ferroperm catalogue 2010).

Polyvinylidene fluoride (PVDF) was considered first as a piezoelectric material because of its high resonance frequency. However, the lack of polarization in the material directed interest to piezoceramics. Ferroperm materials, which are based on Lead

Zirconate Titanate (PZT) were chosen for testing mainly because of their high sensitivity. A piezoceramic with the trade name PZ26 is intended for underwater applications and it was also chosen as the medium used in the filtration.

The piezomaterial was disc shaped and the thickness was chosen to be as small as possible to reach the highest resonance frequency. The diameter of the disc was 5 mm and the thickness 0.2 mm. The material and thickness together determine the resonance frequency to be in the region of 10 MHz. The piezo disc needed a firm backing material, and therefore it was mounted on a printed circuit board (PCB).

Miniaturized coaxial connectors were used to connect to the piezo elements on the PCB. The use of an appropriate coaxial connector was crucial to the quality of the signal. The impedance of the cable was 50 ohm. The other end of the transducer coaxial cable is sub miniature version A (SMA). The coaxial cable and the transducer PCB are shown in Figure 3.3.

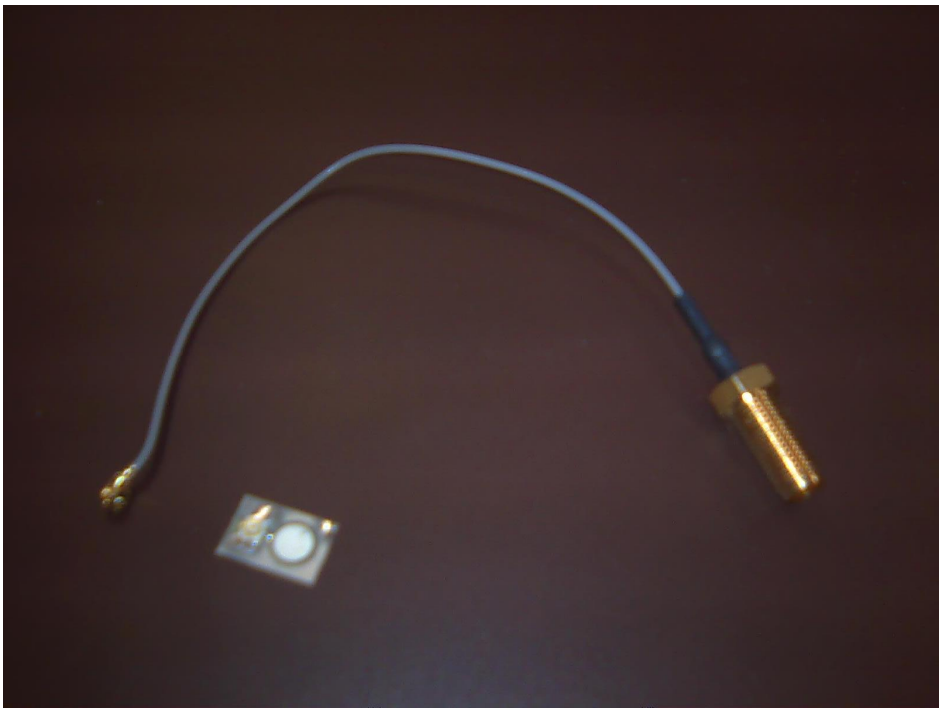

Figure 3.3: Coaxial cable and transducer PCB. Miniaturised coaxial connectors were used to connect to the piezo elements on the PCB (left). The use of an appropriate coaxial cable was crucial to the quality of the signal. The impedance of the cable was 50 ohm. The other end of the transducer coaxial cable is sub miniature version A (SMA) (right).

Instead of soldering connections to the piezo material silver electrodes, a conductive paint consisting mainly of silver was used. This eliminated the risk of piezo material to depolarize.

Figure 3.4 illustrates an opened filter equipment cylinder looking inside from the bottom membrane side. The transducer mounted on the piston measure the distance to the membrane, and the second one, identical mounted to the aluminium u-shaped profile is the reference transducer measuring a fixed distance. Epoxy was used to attach the transducer PCB.

The other end of the transducer coaxial cable SMA was led through the piston. The connectors were sealed up with rubber o-rings so that the cylinder can be pressurized up to 5 bar.

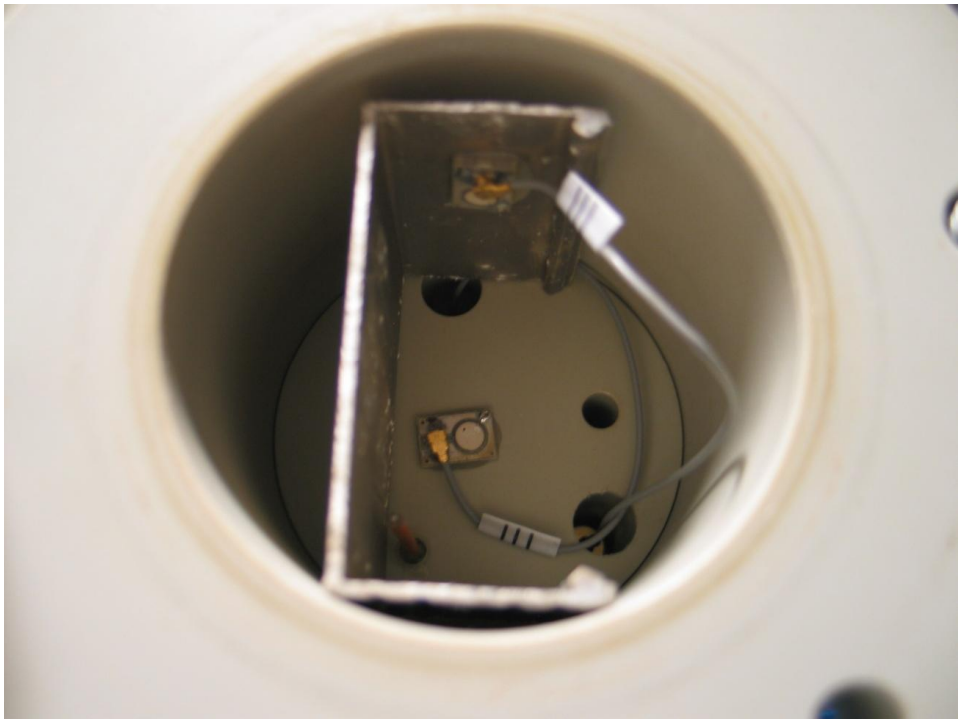

Figure 3.4: Opened filter equipment cylinder looking inside from the bottom membrane side. The transducer mounted on the piston measure the distance to the membrane, and the second identical mounted to the aluminium u-shaped profile is the reference transducer measuring a fixed distance and eliminating the changes in temperature and pressure.

The membrane was placed between the bottom plate and the cylinder. The backing material was mounted to the bottom plate closing the cylinder. The backing material was a stainless steel plate perforated with small holes to sieve the permeate flux through it.

3.2.1 **Reference transducer**

As shown in Section 2.1, when both the pressure and the temperature increase, also the speed of sound increases. If both the pressure and temperature are measured, the speed of sound in water can be corrected with Equations (2.2)–(2.6), and the distance to the membrane surface can be calculated. The accuracy of the system is increased, yet not sufficiently. Both the pressure and temperature measurements have an accuracy of their own, and thereby do not give absolutely correct values. The errors will have an effect on the distance measurements and reduce the resolution.

The speed of sound was calculated with the time values from the reference transducer; the values are shown in the pressure of 1 bar as a function temperature in Figure 3.5. The values were taken at the beginning of the measurement.

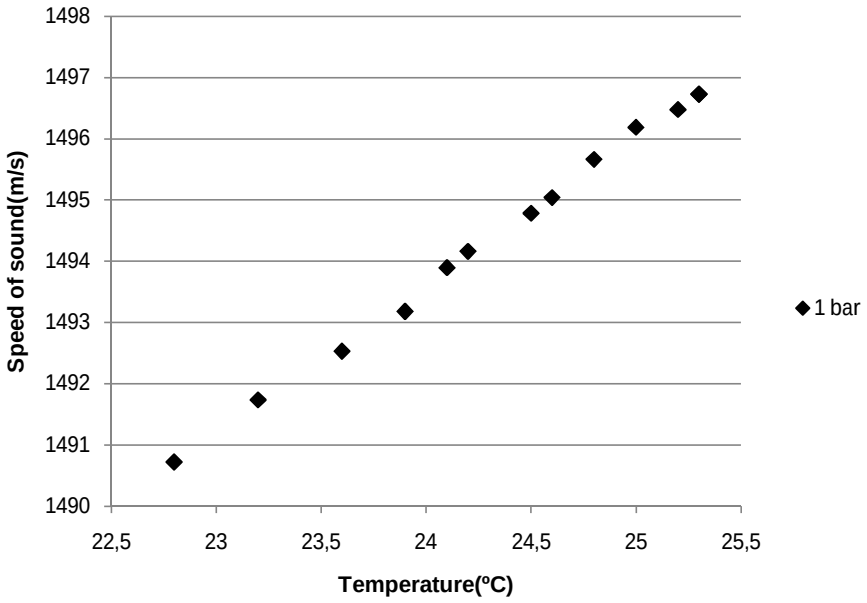

Figure 3.5: Calculated speed of sound obtained by the time values from the reference transducer. Speed in the pressure of 1 bar as a function of temperature. The values were taken at the beginning of the measurement.

The calculated speed of sound obtained by the time values from the reference transducer. Speed in the temperature of 25.5 ºC as a function of pressure is depicted in Figure 3.6.

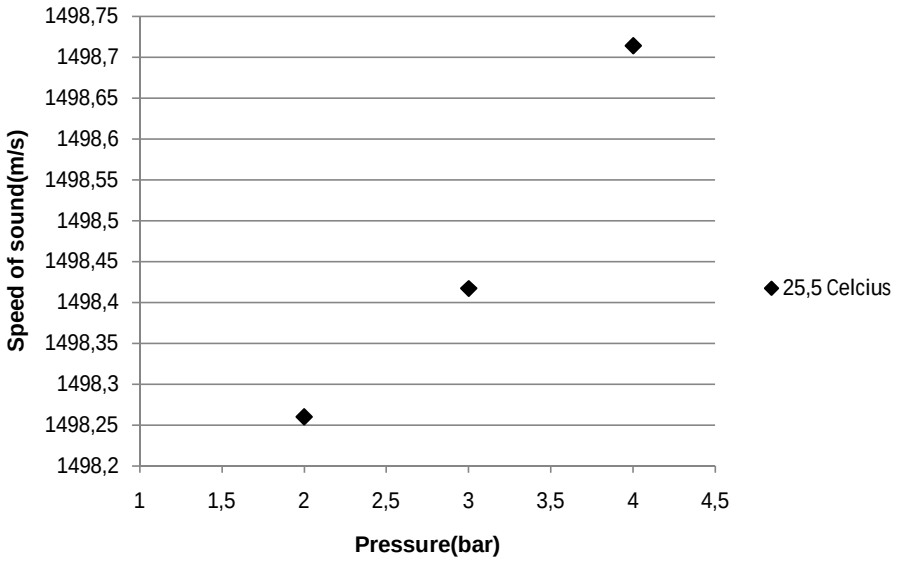

Figure 3.6: Calculated speed of sound obtained by the time values from the reference transducer. Speed in the temperature of 25.5 ºC as a function of pressure.

To eliminate the effect of temperature and pressure change on the speed of sound, a reference transducer is needed. As shown in Figure 3.4, the reference transducer is measuring a fixed distance to the u-shaped aluminium profile. When the time is measured with an oscilloscope and the distance is known, we can calculate the speed of sound in water. This value is then used to calculate the distance to the membrane more accurately.

This method can also be applied to other liquids flowing in the filter, thereby eliminating unwanted phenomena such as change in the pH value or the effect of solvents such as salts. No tabular values of the speed of sound in a certain fluid are required and the method can be used to a variety of fluids containing solvent molecules.

3.3 Waveform generation

The pulser used to make the transducers vibrate at their resonance frequency was an Agilent 33250A Function Waveform generator with a bandwidth of 80 MHz. The pulser was set to make only five sine bursts since the amplitude did not rise significantly after five bursts. The amplitude of the pulser was 10 V peak-to-peak. The frequency was

adjusted to 10.7 MHz, which gave the highest amplitude for the reflected pulse. The termination of the generator output was set to 50 ohm as in the oscilloscope.

The frequency of 10.7 MHz was the resonance frequency of the transducer. The waveform generator was synchronized with the oscilloscope through Bayonet Neill-Concelman (BNC) cables. The oscilloscope was triggered using the sync signal from the waveform generator to keep the time information the same in both devices.

The number of sine bursts was set to five to increase the amplitude of the reflections. Additional bursts magnified the resonance of the piezo element.

3.3.1 **Transducer equivalent circuit**

The electric equivalent circuit for PZ26 piezo element was a series-parallel RLC circuit. Circuit can operate in either series resonance or parallel resonance. An illustration of the equivalent circuit is shown in Figure 3.7.

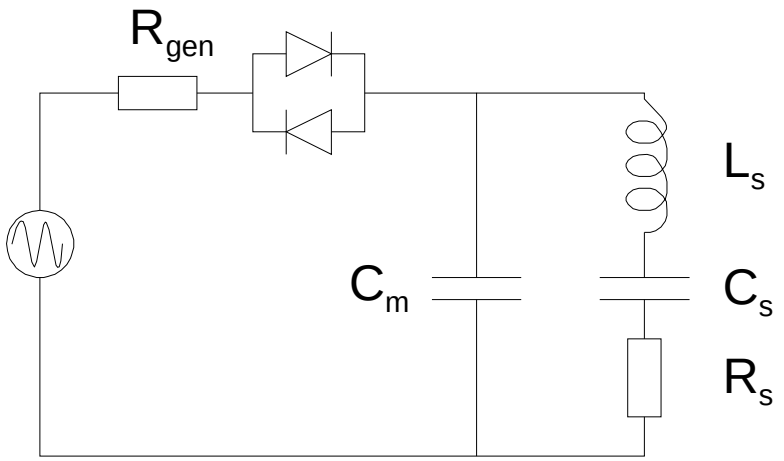

Figure 3.7: Electrical equivalent series-parallel RLC circuit for the PZ26 piezo element. The pulser noise and its output termination R_{gen} were separated by using a diode circuit.

At series resonant frequency, the inductive reactance is cancelled by the reactance of C_s. The remaining series resistor, R_s, determines the impedance of the piezo. Parallel resonance occurs when the inductive reactance and the reactance of the parallel

capacitance, C_m, are equal. The parallel resonant frequency is usually few kHz higher than the series resonant frequency. The pulser noise and its output termination R_{gen} which was 50 ohms were separated by using a diode circuit. (Floyd 2002)

3.4 Time measurement

The oscilloscope used in the measurements was Tektronix TDS3052B with a bandwidth of 500 MHz and a sample rate of 5 GS/s. As the transducer frequency was 10.7 MHz, the bandwidth was more than enough. Nevertheless, a good sample rate is needed to achieve good time resolution for the measurement. The oscilloscope had two channels, and thus it was possible to connect both the membrane transducer and the reference transducer. The pulser synchronization signal was also connected and used to trigger the oscilloscope. The scope was set to average the signal and the input terminal to 50 ohm and the AC coupling.

To accurately measure the time with the oscilloscope, the reflection signal from the membrane surface was zoomed into the section; where the voltage crossed the x-axis in the middle of the screen for the first time. The oscilloscope measured the time from the trigger pulse making the transducer vibrate to the origin of the screen. This way, the time was measured for both of the transducers. As seen in Figure 3.8, the measured time is 77.4579 µs. By applying Equation 2.1, the distance to the membrane surface was calculated using the speed of sound obtained by the reference transducer. To calculate the speed of sound with the reference transducer the fixed distance has to be measured. It was measured in water at 25 ºC in pressure of 1 bar applying the speed of sound from the Belogol'skii equations.

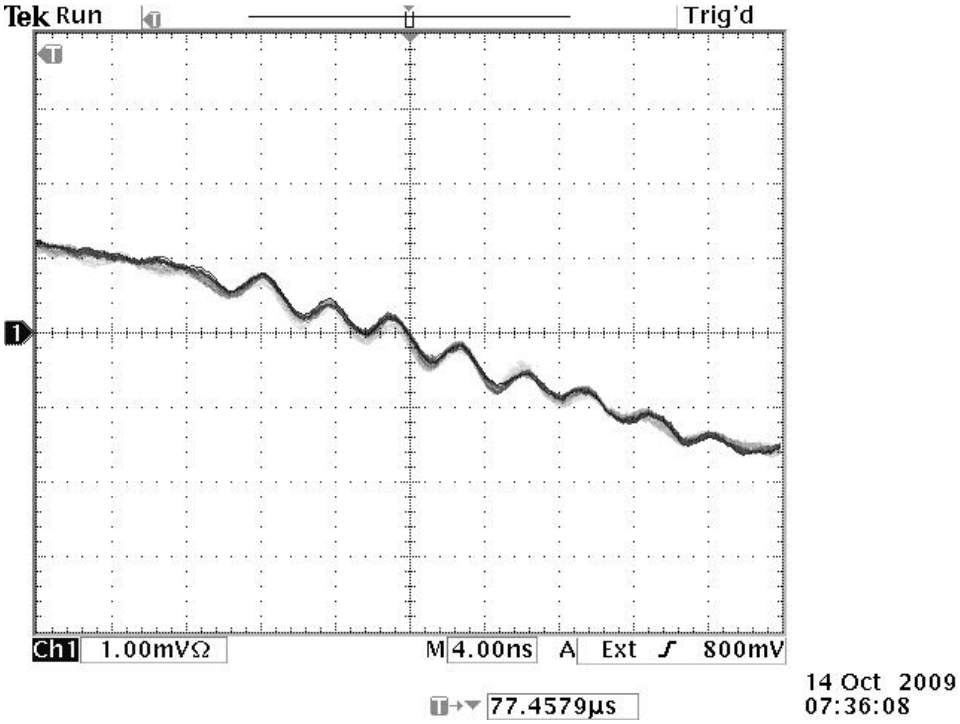

Figure 3.8; Scope zoomed into the section of the reflection pulse, where the voltage crossed the x-axis in the middle of the screen for the first time. The oscilloscope measured the time from trigger pulse making the transducer vibrate to the origin of the screen. The measured time seen at the bottom of the figure is given in microseconds. The distance to the membrane surface was calculated using the speed of sound obtained by the reference transducer.

The oscilloscope time reading as seen at the bottom of Figure 3.8 was within the accuracy of 0.1 ns. The accuracy of the measurement was assumed to be 1 ns, which converted into a distance was of 1 µm. This was gained by applying the equation 2.1 with a constant speed of sound and calculating the difference of distance values when time is 1 ns higher in the other value.

3.5 **Pressure control**

The measurements were carried out in pressures ranging from 1 to 5 bar, and the pressure was raised with a mechanical valve by decreasing the flux of water in the concentrate tube and by increasing the speed of rotation of the pump. The pressure

gauge used was Swagelok gauge with a diameter of 63 mm, and the pressure range was from 0 to 6 bar.

The error defined for the type of the pressure gauge as given by standard EN-837 was ±1.6 % and it was calculated to be ±0.05 µm at 5 bar using the Belogol'skii equations (2.2)–(2.6). (Wika 2010)

Because the effect of the pressure to the error of the distance measurement is very small when using the Belogol'skii equations, the change in the system especially at the lower pressures has to be considered. Figure 3.9 shows the measured distance to the membrane with the reference transducer as a function of pressure between 1-2 bars. The measured pressures are 1 and 2 bar.

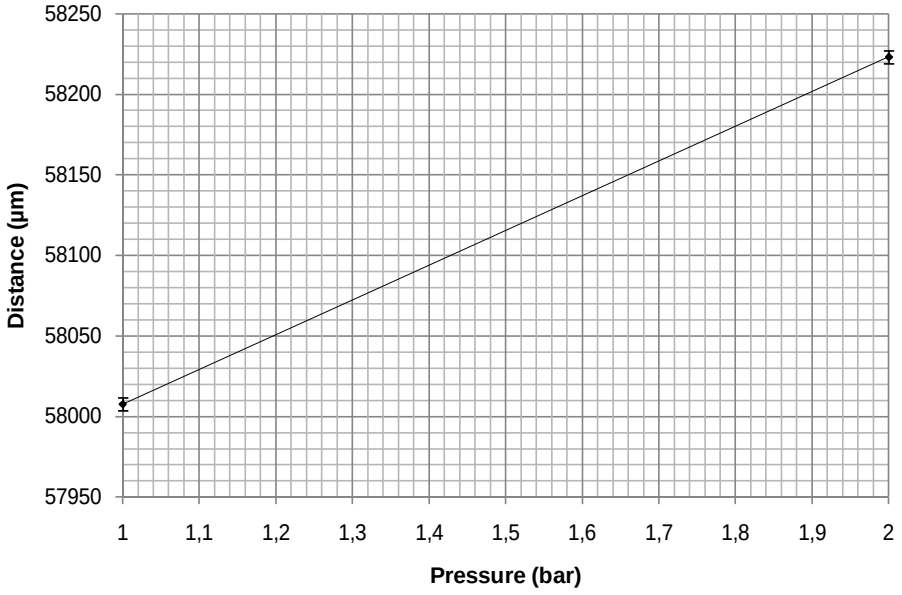

Figure 3.9: Measured distance to the membrane as a function of pressure between 1-2 bars. . The measured pressures are 1 and 2 bar. As seen at the pressure of 1.2 bars the error of ±1.6% corresponds to pressure change of ±0.192 bars which means an error of ±4 µm to the measured distance.

As seen at the pressure of 1.2 bar the error of ±1.6% corresponds pressure change of ±0.192 bars which means an error of ±4 µm to the measured distance. At higher pressures the rate of change in the system is smaller and the error produced smaller as

well. Applying the method describe above errors in the pressures through 1–5 bar are listed in Table 3.1.

Table 3.1: Error caused by the pressure control in pressures through 1–5 bar.

Pressure(bar)	Error due to pressure control(μm)
1	±4.0
2	±3.4
3	±1.7
4	±1.5
5	±1.8

4 Results and discussion

The setup described in Chapter 3 was used to measure the accuracy of system first and the ultrafiltration membrane compaction in pressures of 1–5 bar second. The permeate flux decline was also controlled because it is an indirect indication of the membrane compaction. The thickness of the membrane samples was measured before and after the measurements to confirm the results of compaction. Mechanical compaction measurements using hydraulic piston was made to verify ultrasound measurements. A scanning electron microscope (SEM) was used to analyze the changes in the microstructure of the membranes.

All the samples were treated with an ultrasound bath that uses low–frequency ultrasound to remove any preservatives of the membranes. Ion–exchanged water was used in the treatment, and the water was changed to clean water between baths. This treatment lasted 3 x 10 minutes. After the treatment the samples were stored in the refrigerator until used in the ultrasound measurements. The membranes used were mainly regenerated cellulose membranes with a trade name of UC030T.

4.1 Measurement of accuracy

The accuracy of the system was measured in the pressures through 1 to 5 bar. In each pressure three values of the distance to membrane were taken in a period of 3 minutes. The ultrasound reference transducer was used to calculate the distance accurately. Measured distances are shown in Figure 4.1.

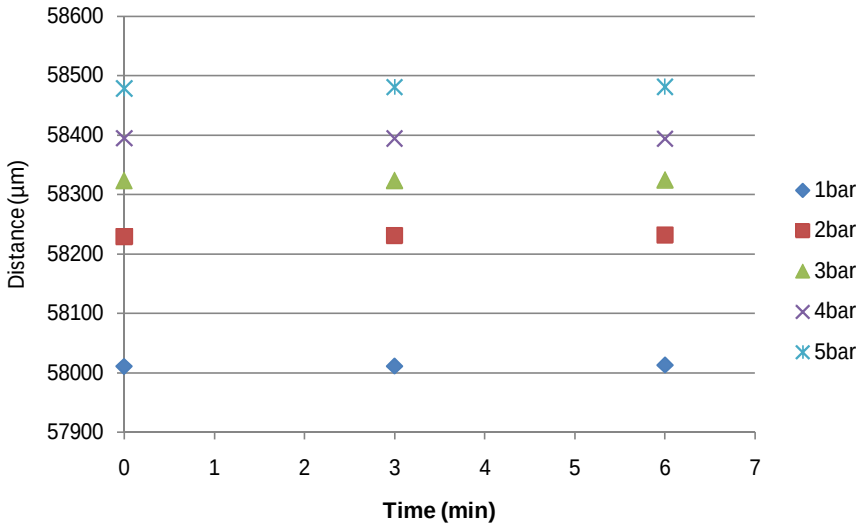

Figure 4.1: Measured distances in different pressures. In each pressure three values of the distance to membrane were taken in a period of 3 minutes.

To solve the accuracy of the ultrasound measurement standard deviation of the measured distances was used to describe the error formed during the measurement. The values for the standard deviation of the measured values in different pressures are shown in Table 4.1.

Table 4.1: Standard deviation of the measured distances. The accuracy of the system is in the range of 1 um.

Pressure(bar)	Standard deviation(µm)
1	1.2
2	1.2
3	0.7
4	0.5
5	1.5

As seen on Table 4.1 the accuracy of the ultrasound system is in the range of 1 µm. Thus, the system can be used to measure changes which are in the range of micrometers.

4.1.1 **Reference transducer measurement vs. Belogol'skii correction**

To show that the reference transducer improves the accuracy of the ultrasound system, distance to the membrane was measured with and without the reference transducer. The same membrane sample was measured through the pressures of 1 to 5 bars and the membrane was held 1 hour in the pressure of 1 bar to let the membrane settle before making distance measurements.

The error produced by the temperature gauge reading to the Belogol'skii measurement was ±0.1 ºC. Temperature error in the distance measured was ±10 µm applying the Belogol'skii equations. Both measurements also suffered from the error produced by the pressure control as shown in Table 3.1. The error of the Belogol'skii measurement is the square root of the error squares. The error bars in different pressures for the reference transducer measurement were as in Table 3.1 and the errors for the Belogol'skii measurement are shown in Table 4.2.

Table 4.2: Error of the Belogol'skii measurement in pressures through 1–5 bar. Error from the temperature reading and the pressure control together.

Pressure(bar)	Error of the Belogol'skii measurement (µm)
1	±11
2	±11
3	±10
4	±10
5	±10

The measured distance in pressure of 1 bar with the reference transducer was compared to the measurement applying the Belogol'skii equation as shown in Figure 4.2.

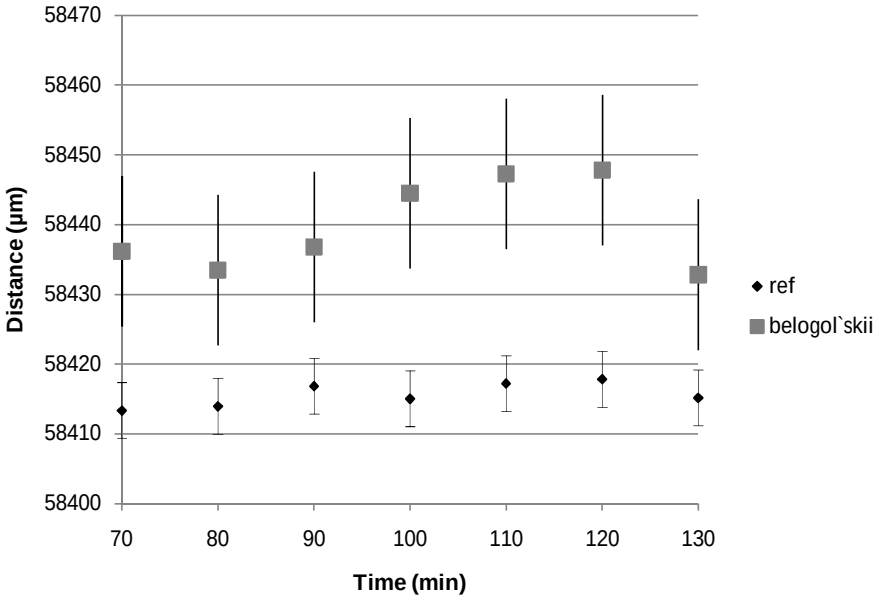

Figure 4.2: Distances measured to the membrane in pressure of 1 bar with the reference transducer and without it applying Belogol'skii equations to correct the effect of the temperature. The accuracy achieved with reference transducer is higher.

As seen in the Figure 4.2 the accuracy of the distance measurement with the reference transducer is higher than the measured distance without the reference transducer applying the Belogol'skii equations to correct the effect of the temperature to the speed of sound. Temperature values for the each measurement in pressures through 1–5 bars are shown in Appendix A.

The accuracy comparison for the distance measurement was repeated in the pressure of 2 bar. The measured distances with both methods are show in Figure 4.3.

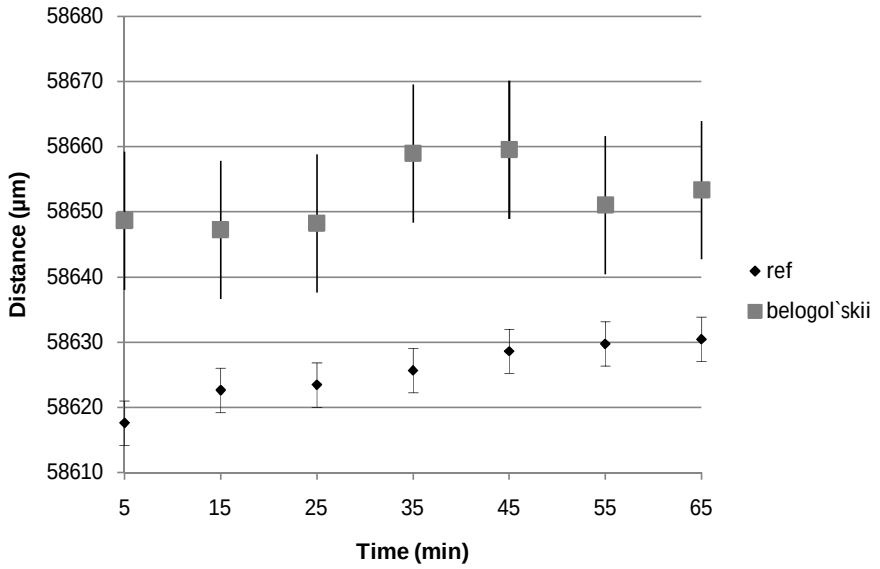

Figure 4.3: Distances measured to the membrane in pressure of 2 bar with the reference transducer and without it applying Belogol'skii equations to correct the effect of the temperature. The accuracy achieved with reference transducer is higher.

As the pressure is raised the filter module expands so the distance measured with the ultrasound increases. As seen on Figure 4.3 deviation in the measured distance values is lower when reference transducer is used.

The accuracy comparison for the distance measurement was again repeated in the pressure of 3 bar. The measured distances with both methods are show in Figure 4.4.

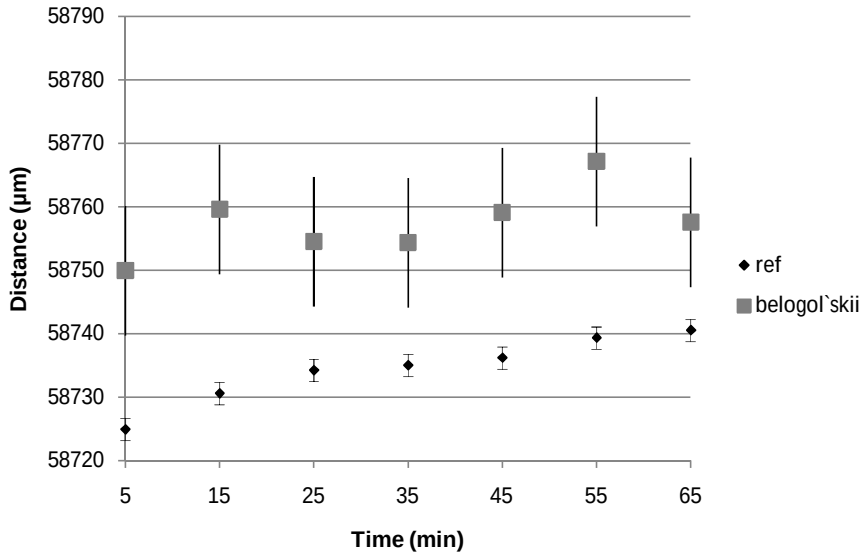

Figure 4.4: Distances measured to the membrane in pressure of 3 bar with the reference transducer and without it applying Belogol'skii equations to correct the effect of the temperature. The accuracy achieved with reference transducer is higher.

The variation in the measured distance values without the reference transducer is higher. The accuracy achieved with the reference transducer much better than applying Belogol'skii equations to correct the changes in temperature. The measured distances in pressure of 4 bars are shown in Figure 4.5.

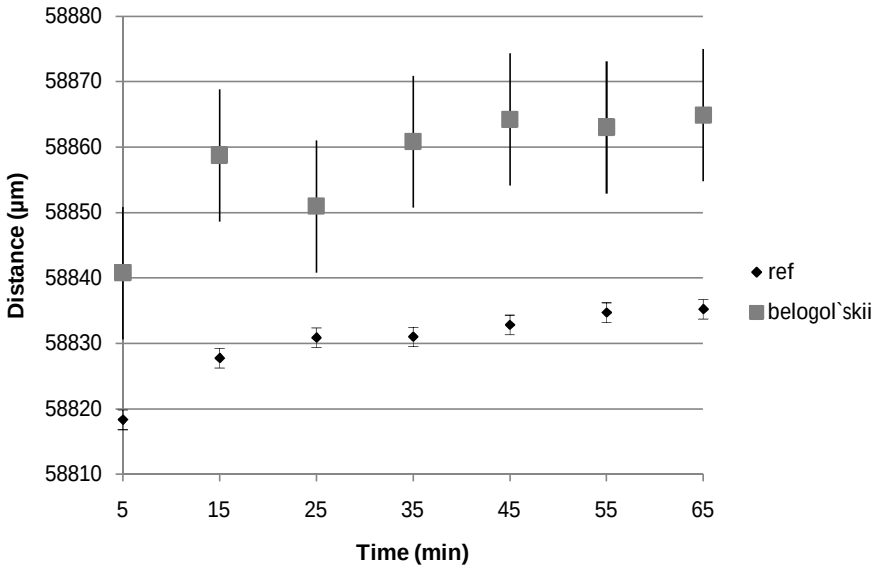

Figure 4.5: Distances measured to the membrane in pressure of 4 bar with the reference transducer and without it applying Belogol'skii equations to correct the effect of the temperature. The accuracy achieved with reference transducer is higher.

Again the accuracy with the reference transducer is higher. The measured distances in pressure of 5 bars are shown in Figure 4.6.

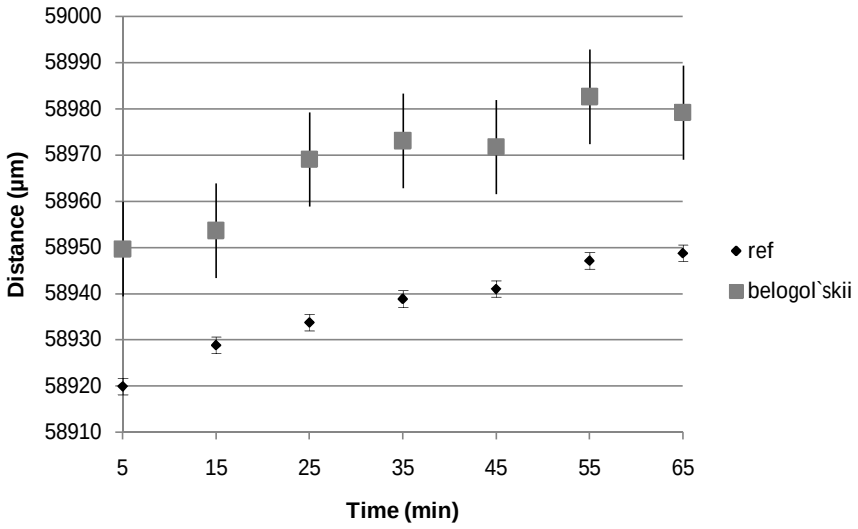

Figure 4.6: Distances measured to the membrane in pressure of 5 bar with the reference transducer and without it applying Belogol'skii equations to correct the effect of the temperature. The accuracy achieved with reference transducer is higher.

At the pressure of 5 bar the variations in the measured distances applying Belogol'skii equations are smaller than in lower pressures. Although the variations are higher than with distances measured using the reference transducer.

As proven in the results of the measured accuracy of the developed ultrasound reference transducer measurement, it is evident that such a system is needed when measuring changes in the ranges of micrometers.

4.1.2 Reference transducer measurement vs. without correction

In many of the earlier researches, as described in the introduction, the speed of sound in the water is assumed to be constant in the temperature used. Usually the temperature change is reported to be ± 1 ºC. The following measurements show the variations in the measured distance values when the reference transducer measurement developed in this thesis is used and without it assuming that speed of sound is constant through out pressures of 1 to 5 bars.

The same membrane sample as in previous chapter measured through the pressures of 1 to 5 bars and the membrane was held 1 hour in the pressure of 1 bar to let the membrane

settle before making distance measurements. The speed of sound used for the measured distances without the reference transducer is 1498 m/s which is the speed of sound in temperature of 25 ºC and in the pressure of 1 bar. Temperature values for the each measurement in pressures through 1–5 bars are shown in Appendix A.

The error bars applied for the reference transducer measurement as shown in Table 3.1. The error bars for the measurement without correction was calculated as in Chapter 4.1.1 meaning that ±0.1 ºC change in temperature yields an error in the distance measurement of ±10 µm. Temperature variations for each pressure were applied and the values for total error are listed in Table 4.3.

Table 4.3: Error of the measurement without correction. Error from the temperature change and the pressure control together.

Pressure(bar)	Error of the Belogol'skii measurement (µm)
1	±30
2	±15
3	±15
4	±30
5	±20

The distances measured to the membrane in 1 bar with the reference transducer and without it assuming the speed of sound to be constant are shown in Figure 4.7.

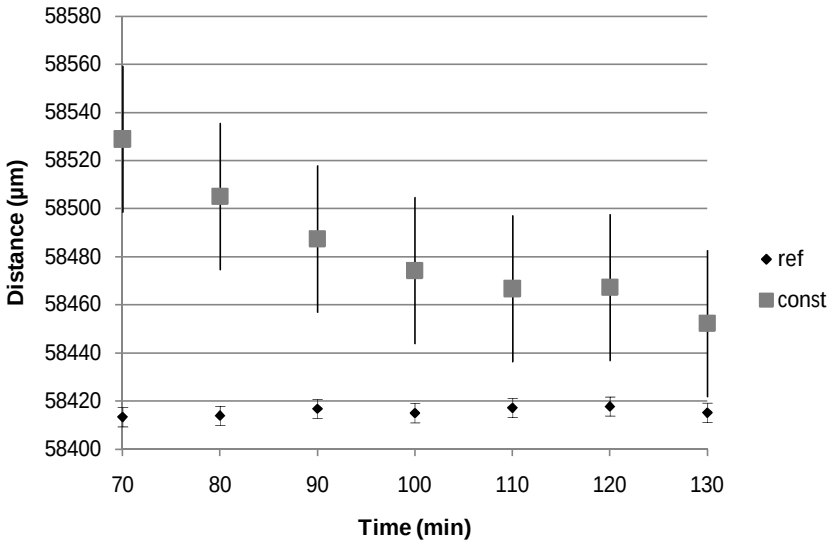

Figure 4.7: Distances measured to the membrane in 1 bar with the reference transducer and without it assuming the speed of sound to be constant. As seen in the beginning of the measurement temperature has not yet reached 25 ºC therefore the speed of sound is lower than assumed and the measured distance higher. The accuracy achieved with reference transducer is higher.

As seen in the beginning of the measurement the temperature has not yet reached 25 ºC therefore the speed of sound is lower than assumed and the measured distance higher. The temperature change is corrected in the measurement with the reference transducer and the effect of the temperature change is eliminated and the distance measured with higher accuracy.

The accuracy comparison for the distance measurement was repeated in the pressure of 2 bar. The measured distances with both methods are show in Figure 4.8.

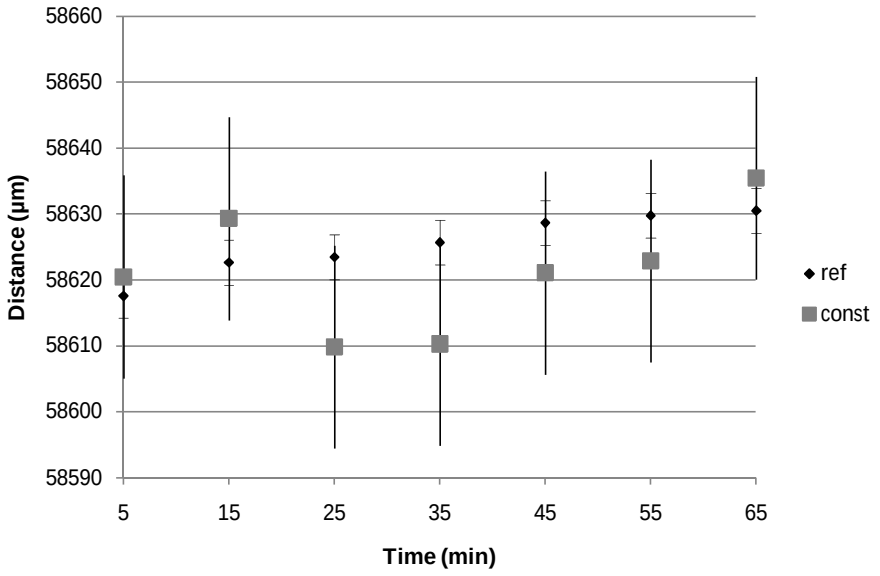

Figure 4.8: Distances measured to the membrane in 2 bar with the reference transducer and without it assuming the speed of sound to be constant. The accuracy of distance measurement applying reference transducer is higher.

In the pressure of 2 bar the temperature is settled to 25 ºC but even small changes in temperature increase the error of measurement without the reference transducer.

The accuracy comparison for the distance measurement was again repeated in the pressure of 3 bar. The measured distances with both methods are show in Figure 4.9.

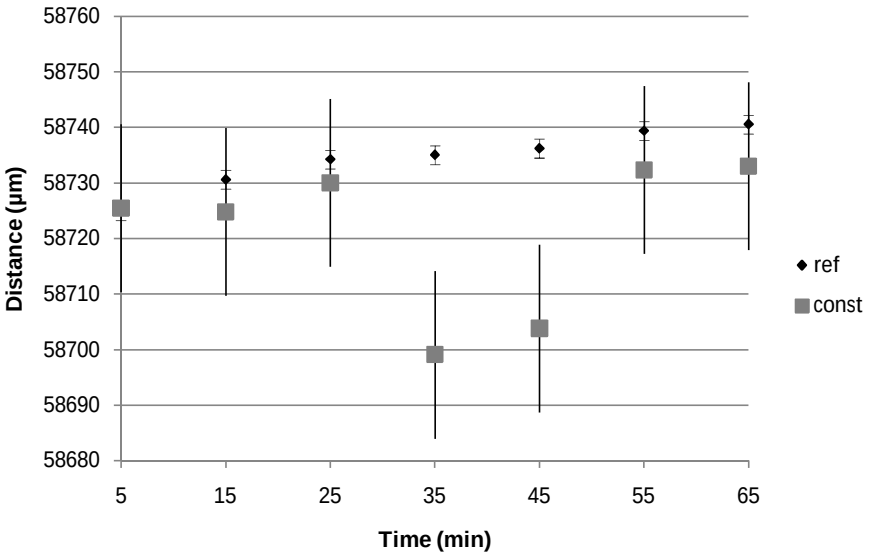

Figure 4.9: Distances measured to the membrane in 3 bar with the reference transducer and without it assuming the speed of sound to be constant. The accuracy of distance measurement applying reference transducer is higher.

In Figure 4.9 the method relying on the constant speed of sound in water cause error of nearly 30 µm to the measured distance. The measured distances in the pressure of 4 are shown in Figure 4.10.

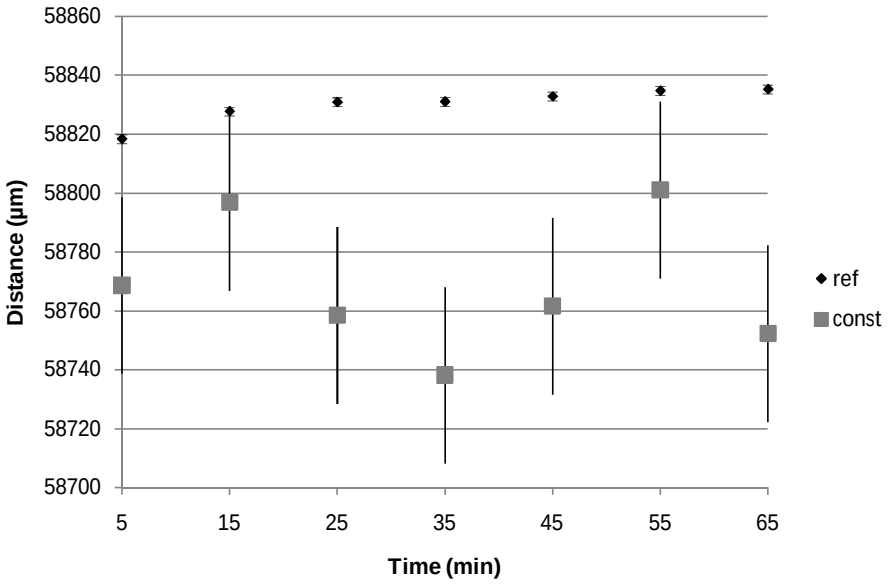

Figure 4.10: Distances measured to the membrane in 4 bar with the reference transducer and without it assuming the speed of sound to be constant. The accuracy of distance measurement applying reference transducer is higher.

As the pressure is increased and the temperature reaches 26 ºC the speed of sound is increased. The measured distance based on constant speed of sound is smaller that with the method applying the reference transducer. Also the variation in the values is high because temperature change is not eliminated. The accuracy comparison in the pressure of 5 bars is shown in Figure 4.11.

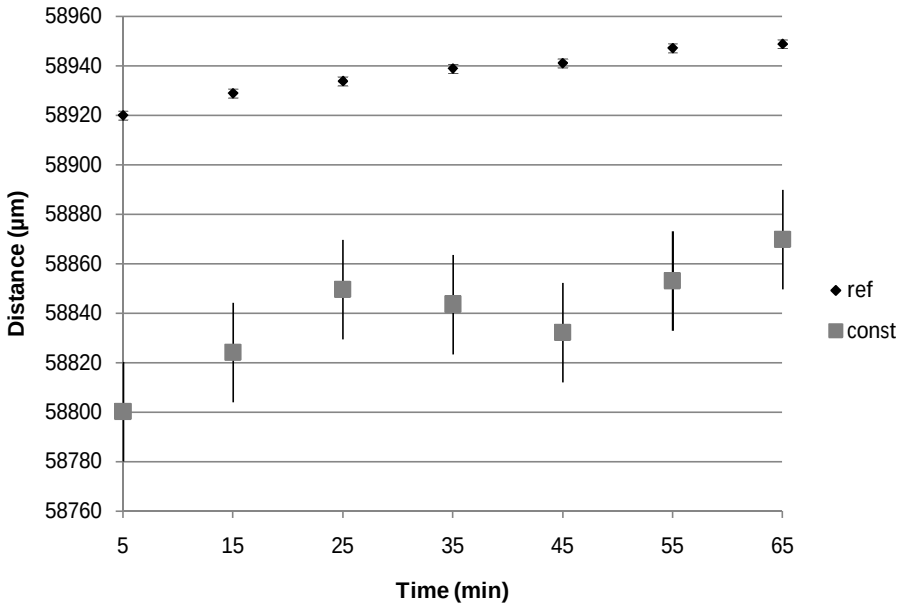

Figure 4.11: Distances measured to the membrane in 5 bar with the reference transducer and without it assuming the speed of sound to be constant. The accuracy of distance measurement applying reference transducer is higher.

When the pressure is further increased more systematic error is produced to the measured distance when the speed of sound is assumed constant. Also the variation in the values is high because temperature change is not eliminated by the reference transducer. According the measurements presented above it is distinctive that the reference transducer is needed to accurately measure distances in filters where both the pressure and temperature change.

4.2 Eliminating filter module changes

After numerous test runs, it was evident that the filter module expanded when a higher pressure was applied. To eliminate this effect, a distance measurement with a thin aluminium foil in place of membrane was made at the pressures from 1 to 5 bar applying the same procedure as in the membrane measurements. The thickness of the aluminium foil was 35 µm, and it was assumed that the compaction of the foil was so small that it could be neglected. The distance measurement with the foil in different pressures was the change in the filter module distance.

4.3 Ultrasound membrane changes

After eliminating the changes in the filter module, the ultrasound measurements for the membrane were carried out in the same way. The measurement of the membrane compaction with ultrasound was made with the membrane between the cylinder and the bottom plate. The bottom plate was then tightened with a momentum of 15 Nm to keep the cylinder in the same position between the different membrane samples. The membrane was against the stainless steel plate, which was perforated with small holes. This backing material supported the membrane structure and was able to sieve water through it.

The water tank was then filled with ion–exchanged water to keep the filter as clean as possible. The pump was started and the air in the filter was replaced with water. Before the experiment started, the filter was held one hour in the pressure of one bar to let the membrane find its place against the backing plate. The time values for both transducers were read as described in Section 3.4 and written down every 10 minutes during the preparation of the membrane.

After the preparation of the membrane, the distance to the membrane surface was measured for one hour in the pressure of 1 bar, and the time values of both transducers were written down every 10 minutes. Also the permeate flux through the membrane was measured and written down every 10 minutes. The permeate flux was measured by weighting the water coming through the membrane in one minute. The procedure was then repeated for the pressures of 2–5 bar. Higher pressures also increased the temperature, and therefore ice frozen from ion–exchanged water was applied to the water tank to cool it down.

The experience gained from the earlier test runs indicated that the temperatures inside the filter and in the water tank are different when a higher pressure is applied. The need for temperature measurement in both places was reasonable. The change in the temperature in the filter does not affect to the distance measurements because of the reference transducer eliminating the effect as described in Section 3.2.1. The temperature is still an important factor in filtration as it affect to the characteristics of the membrane, and so it was monitored. The temperature measured in the water tank and in the filter as a function of pressure is shown in Figure 4.12.

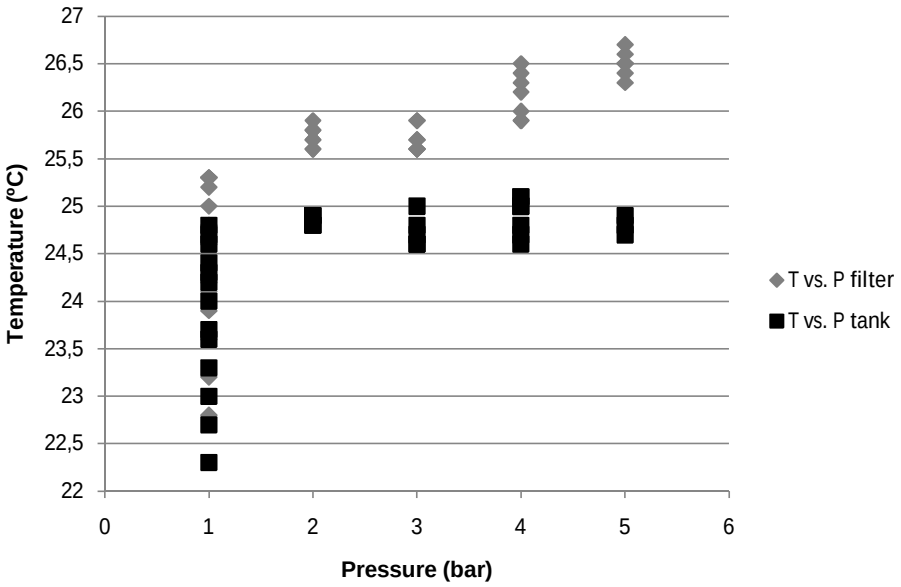

Figure 4.12: Temperature measured in the water tank and in the filter as a function of pressure. The temperature rises in the filter when a higher pressure is applied.

At higher pressure the concentrate flux was decreased with the mechanical valve. This forced water to flow more through the membrane and not freely from the concentrate line and the temperature rose.

After the measurement of the membrane with ultrasound, the results were compared with the thin aluminium foil measurements. The change between the distances of these two measurements as a function of pressure was analyzed to be the membrane compaction. The average of two last values in each pressure was used for the distance. Figure 4.13 presents the distance of the membrane and the foil as a function of pressure.

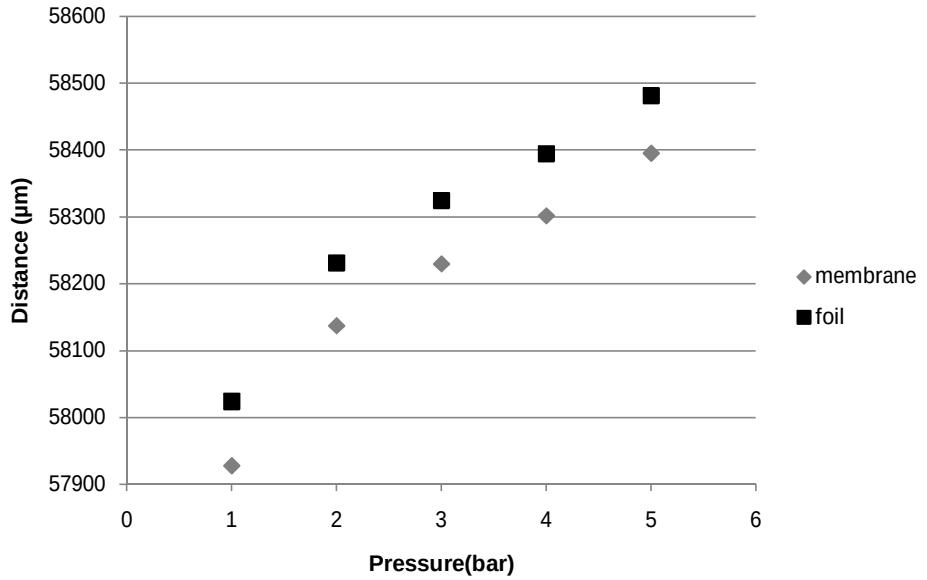

Figure 4.13: Distance of the membrane and the aluminium foil as a function of pressure. The change in distances of these two measurements as a function of pressure was analyzed to be the membrane compaction.

As seen on figure 4.13 the distance measured increases as the pressure is increased. This system change will cause that the pressure has to be controlled very accurately to achieve measurements that can be compared with each other.

The graphs for distances in Figure 4.13 do not start at the same point because the thickness of the membrane and the foil is different and the filter location changes when it is opened and closed between the samples. This means that the change in distances has to be used not the absolute values for distances.

Since compaction values are combination of aluminium foil distance measurement and membrane distance measurement the error caused by the pressure control is therefore combined. Error in different pressures for compaction values is the square root of the squares presented in Table 3.1 and are listed again in Table 4.4.

Table 4.4: Error caused by the pressure control in pressures through 1–5 bar to the compaction values.

Pressure(bar)	Error due to pressure control(µm)
0.5	±5.7
1	±5.6
2	±4.9
3	±2.5
4	±2.1
5	±2.5

First, the membrane UC030T was measured with two samples 1 and 2. The compaction of these membranes is illustrated in Figure 4.3. Error bars for both of the membranes as listed in Table 4.4 in different pressures.

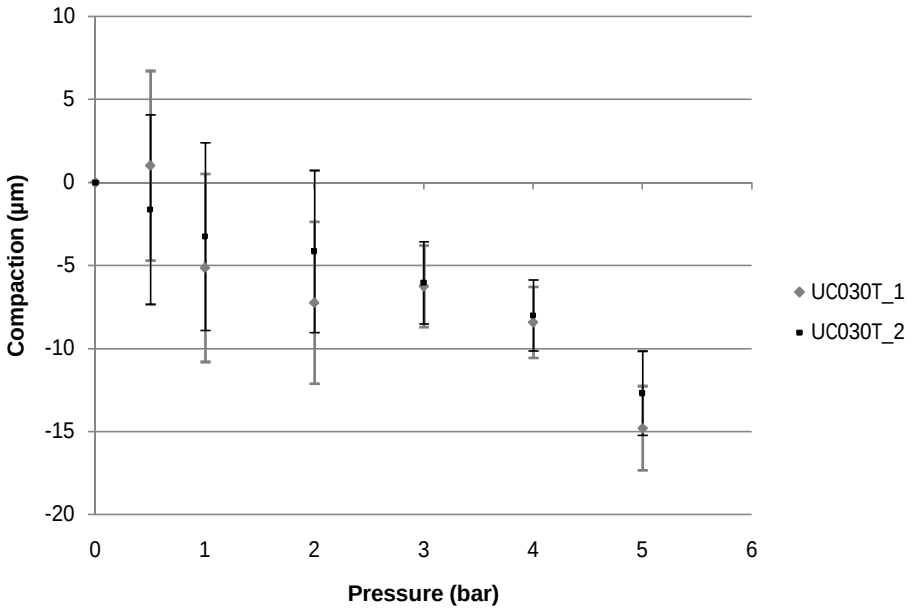

Figure 4.14: Compaction of sample 1 and 2 UC030T membranes as a function of pressure.

For these membranes, the values at 0.5 bar were the last ones measured and, the compaction at 0 bar, which is the pressure in atmosphere, was linearly extrapolated to be 0 µm. The maximum value for the compaction of UC030T sample 1 in the pressure of 5 bar is approximately 15±2.5 µm. The maximum value for the compaction of UC030T sample 2 in the pressure of 5 bar is approximately 13±2.5 µm. The compaction values for both membrane in each pressure are inside the error bars. These samples were not analyzed with a micrometer or an SEM, because they idea to back up results was discovered later.

The experiment was repeated for UC030T samples A and B. The compaction of these membranes is shown in Figure 4.15. The measured values for sample A are presented in Appendix B the values were written down by hand, because automated measurement control was not used.

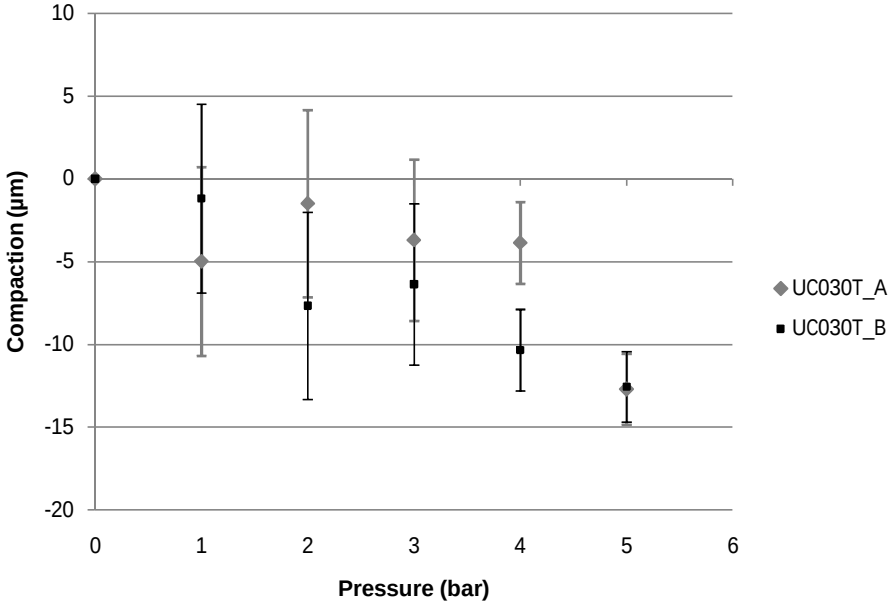

Figure 4.15: Compaction of sample A and B UC030T membranes as a function of pressure.

The maximum, compaction in samples A and B is 13±2.5 µm. Although sample A differs from B, at lower pressures due to lower accuracy in the pressure control the maximum compaction in both is the same. The compaction measured in 5 bar in samples 1 and 2 is inside the error bars of the measurement with the samples A and B. The measured values for compaction would not be seen without the reference transducer which significantly improves the accuracy of the ultrasound measurement.

4.3.1 **Discussion**

The maximum compaction of the UC030T membrane using ultrasound reflectometry as seen in Figure 4.14 is 15±2.5 µm for sample 1 and 13±2.5 µm for sample 2. The same membrane type is used in the ultrasound measurements for samples A and B. The maximum compaction is approximately 13±2.5 µm for both samples. Although there is deviation at the beginning, because of lower accuracy in the pressure control the maximum values are the same for samples A and B. The results correlate between samples 1 and 2, because measured values are inside the error bars of the sample A and B. This shows that the experiment is repeatable. In all of the four samples, the

maximum compaction is nearly the same showing that the repeatability and reliability of the experiment is evident.

As proven earlier chapters the need for reference transducer to eliminate the effect of temperature and pressure and achieve higher accuracy is evident. Although the accuracy is high enough to measure the compaction. As proven in the earlier chapter the accuracy of ultrasound measurement itself has accuracy within 1 micrometer.

4.4 Permeate flux decline

Permeate flux decline is an indication of membrane compaction. The flux increases as the pressure is higher. Permeability describes better the efficiency of the membrane and is defined as the flux divided by the membrane area and the pressure used. In Figure 4.16, the compaction of samples A and B is plotted together with the permeability of the membrane through pressures from 2 to 5 bar.

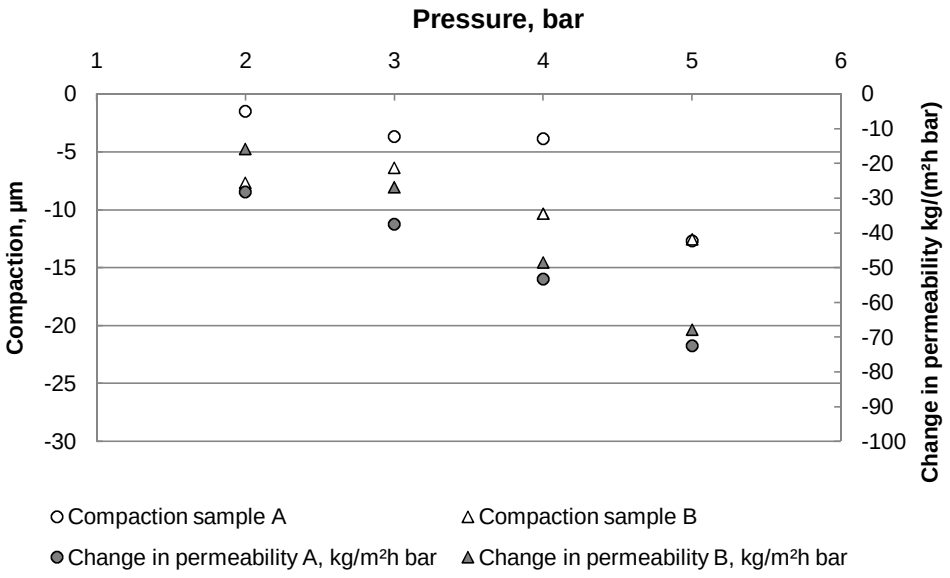

Figure 4.16: Compaction and pure water permeability of samples A and B as a function of pressure.

As seen in Figure 4.16, the change in permeability of the samples decreases when the compaction increases. This result is convergent with the compaction measurements using ultrasound.

4.4.1 **Discussion**

To back up the compaction measurements using ultrasound, the flux in samples A and B was measured throughout the experiment. The reason for this is that the permeate flux decline of the filter is an indication of membrane compaction. The flux increases as the pressure increases. Permeability describes better the efficiency of the membrane and is defined as the flux divided by the membrane area and the pressure used. As seen in Figure 4.16, the change in permeability of the samples decreases when the compaction increases, confirming that the compaction has occurred.

4.5 **Micrometer thickness results**

To evaluate the ultrasound measurements of membrane compaction, samples A and B were measured using a micrometer. The thickness of the samples was measured when dry, wet after the treatment with ultrasound, wet before the measurements, wet after the measurements and once again in the morning following the measurement day to find out if the compaction was recoverable.

The thickness of the membrane was measured with a Lorentzen&Wettre micrometer with an accuracy of ±1 µm. The micrometer fulfilled the standard SCAN-P 7:96 for measuring the thickness in paper and board. As described in the standard micrometer used static force of 20 N on the area of 200 mm^2 which converted into pressure is 100 kPa or 1 bar. The values were taken from three different places of the membrane, and the average of them was used. The compaction is the difference between the wet–before and wet–after values. The results are given for the UC030T sample A in Table 4.5.

Table 4.5: Micrometer results for the compaction of the membrane UC030T sample A. Values in µm.

UC030T sample A	1	2	3	average	compact.	recovery
dry	224	230	223	226		
wet before	234	229	226	230		
wet after	210	207	203	207	23	
wet next morning	211	214	208	211		4

The compaction of sample A is 23 µm and the recovery of the membrane 4 µm. The second sample B was measured in the same way, and the results are shown in Table 4.6.

Table 4.6: Micrometer results for the compaction of the membrane UC030T sample B. Values in µm.

UC030T sample B	1	2	3	average	compact.	recovery
dry	241	242	240	241		
wet before	240	250	243	244		
wet after	219	217	218	218	26	
wet next morning	218	221	220	220		2

The compaction of the second sample B is 26 µm and the recovery of the membrane is 2 µm. As seen on the measured thicknesses the material is heterogeneous so average was used to calculate the compaction.

4.5.1 **Discussion**

To verify the ultrasound measurements of the membrane compaction, samples A and B were measured using a micrometer. The thickness of the membrane was measured with a Lorentzen&Wettre micrometer with an accuracy of ±1 µm. The values were measured from three different places of the membrane, and the average of them was used. The compaction is the difference between the wet–before and wet–after values. The results for the UC030T sample A in are given in Table 4.5.

The second sample B was measured in the same way, and the results are shown in Table 4.6. The sample A compaction was measured to be 23 µm, and for sample B 26 µm. The samples were stored in refrigerator and the thickness was measured again next morning. The recovery of the membranes was measured to be 2–4 µm.

The difference between the ultrasound measurements and the micrometer results is noticeable. As seen on Table 4.6 the variation between measured thicknesses wet before the membranes is 10 µm, which indicates that membranes are very heterogeneous. Micrometer results are averages of three measured values and ultrasound measures one section of the membrane. This might be the reason behind the variation in results between ultrasound and micrometer. Also the measuring pressure of the micrometer might increase the values measured for the compaction of membrane. However, the main result from the micrometer is that the compaction has occurred.

4.6 Mechanical compaction using a hydraulic piston

The compaction of the UC030T membrane was also measured with a hydraulic piston at the Department of Mechanical Engineering. The force applied was controllable and the position of the piston was measured with a probe measuring the shift of the piston. The measurement setup is shown in Figure 4.17.

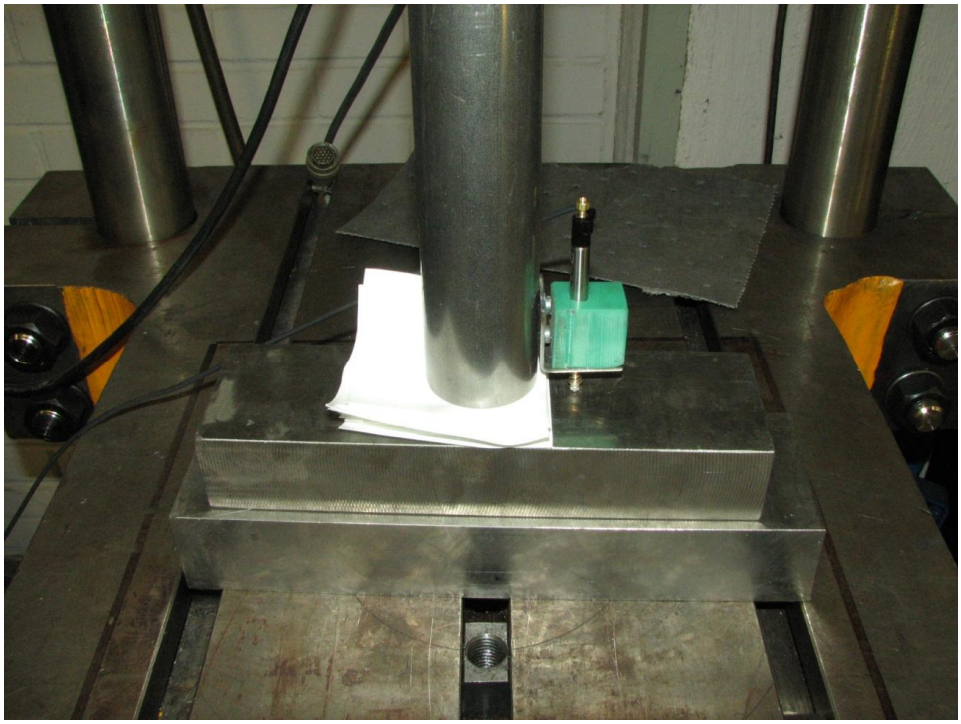

Figure 4.17: Compaction of the UC030T membrane measured with a hydraulic piston. The force applied was controllable and the position of the piston was measured with a probe measuring the shift of the piston.

The diameter of the piston was known to be 50 mm and the force was in newtons. The force values were converted to pressure values by dividing them by the area of the piston. Because of the accuracy of the system, measurement of only one membrane was not possible, and therefore 40 membrane samples stacked together were used. The point where the stack of membranes started to resist the applied force was taken as the zero compaction point.

The values for the shift were then divided by the number of membrane samples to get the compaction of one membrane. The compaction of the membrane is shown as a function of pressure in the Figure 4.18.

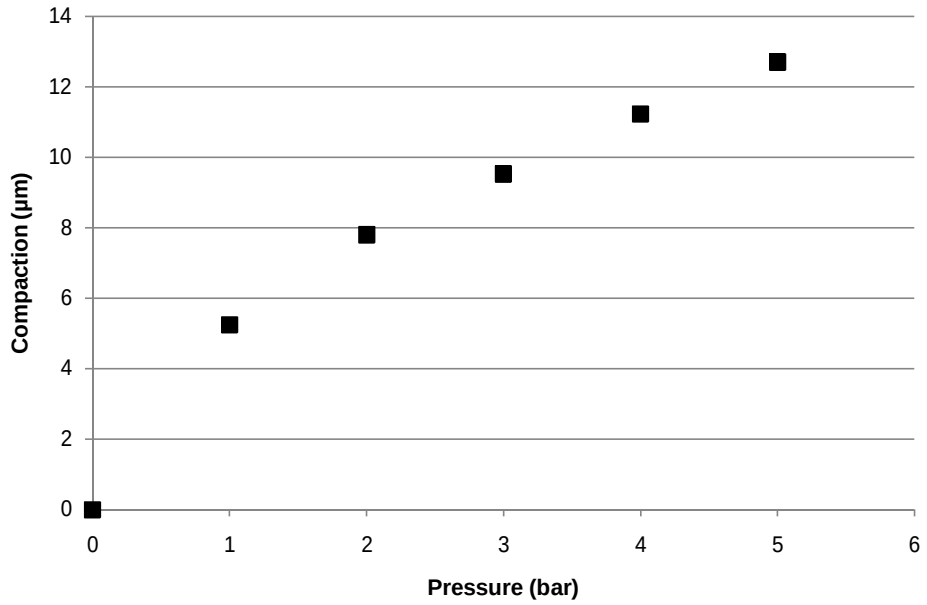

Figure 4.18: Mechanically measured compaction of the UC030T membrane as a function of pressure.

At the force equivalent to a pressure of 5 bar, the compaction was measured to be 13 µm. The results for the total compaction are the same as using the UTDR.

4.6.1 **Discussion**

The compaction of the UC030T membrane was measured with a hydraulic piston. The force applied was controllable and the position of the piston was measured with a probe measuring the shift of the piston. Because of the accuracy of the system, measurement of only one membrane was not possible, and therefore 40 membrane samples were used. The compaction of the membrane is shown as a function of pressure in Figure 4.18. At the force equivalent to pressure of 5 bar, the compaction was measured to be 13 µm. The results for the total compaction are the same as using the UTDR. Thus, these results confirm that the results obtained by the UTDR are reliable.

4.7 SEM analysis

A scanning electron microscope (SEM) was used to analyze the layer structure of the membranes after the ultrasound measurements. The objective was to find out what happens in the layer structure when the compaction occurs. The surface and the porous intermediate layer of the UC030T membrane are known to be regenerated cellulose. The fibered support layer consists of polyethylene terephthalate (PET). The layer structure of the virgin UC030T is seen in the SEM cross–section image shown in Figure 4.19. (Kallioinen 1/2007)

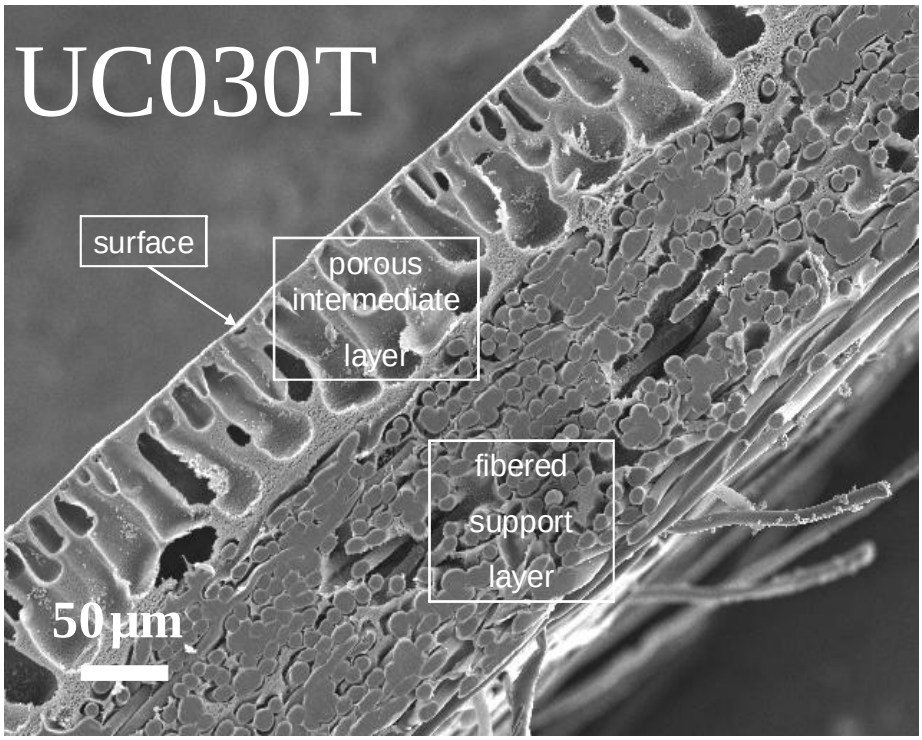

Figure 4.19: SEM cross-section image of the layer structure of the virgin UC030T ultrafiltration membrane. The surface and the porous intermediate layer of the UC030T membrane is regenerated cellulose. The fibered support layer consists of polyethylene terephthalate (PET). (Kallioinen 1/2007)

Total thickness of the virgin sample analyzed with SEM is 250 µm. The thickness of the porous intermediate layer is 89 µm. Thickness of the fibered support layer is 161 µm.

All the samples examined with the SEM had to be dry and coated with an electrically conducting material. The cross-section samples of the membranes were cut with razor blade and they were sputtered using gold which formed thin electrically conducting coating on them.

The SEM used was JEOL JSM-5800 placed at the Department of Chemistry. A SEM is an electron microscope that images the sample surface by scanning it with a high-energy beam of electrons row by row. Accelerating voltage for electrons was 10 kV and the operation distance used was set to 15 mm.

The electrons interact with the sample atoms, producing signals that contain information about the sample structure. Secondary electron imaging (SEI) was used in the SEM to produce a high–resolution image of the sample surface. A benefit of the SEM is that it can point out details in the nanometre range because of the narrow electron beam, and the micrographs also have a large depth of yield; thus the 3D appearance is useful for understanding the structure of the sample.

A wide range of magnifications is possible, from about 10 times to more than 500,000 times, which is about 250 times the magnification limit of the best light microscopes. These characteristics make the SEM a versatile tool for analyzing membrane samples.

The sample A which was used in the UTDR measurements and pressurized through 0 to 5 bars was fully dried and analyzed with the SEM. SEM cross-section image of the layer structure is shown in Figure 4.20.

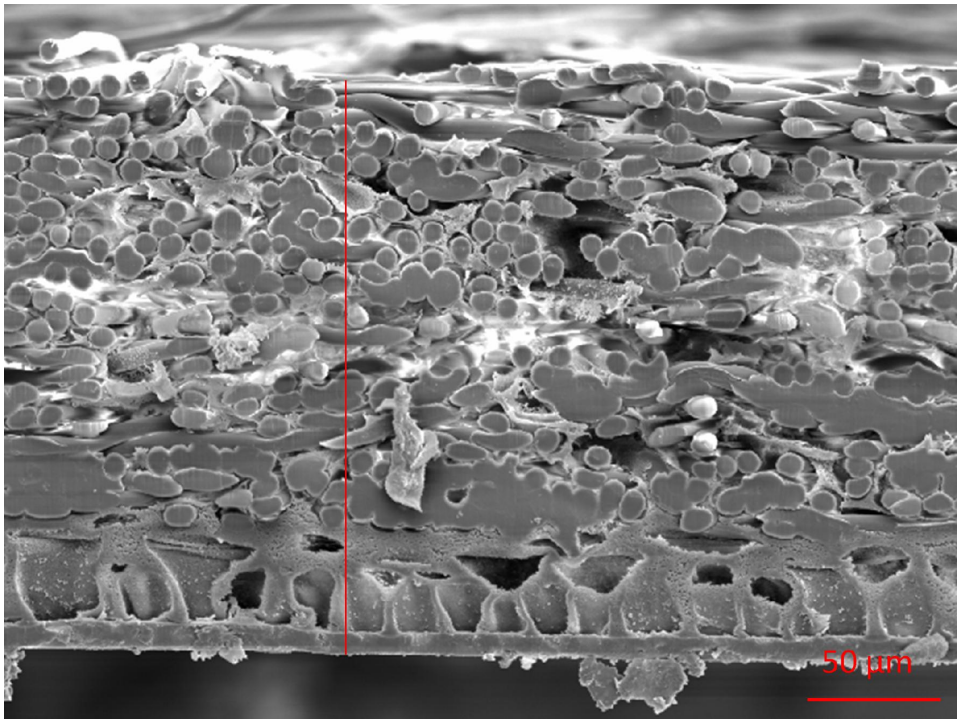

Figure 4.20: SEM cross-section image of the layers structure of the UC030T membrane sample A pressurized through 0 to 5 bar in UTDR measurement.

Total thickness of the compacted membrane is 218 µm the thickness of the porous intermediate layer is 48 µm and support layer 171 µm. As seen on the Figure 4.20 the porous intermediate layer seems more flatten than in the virgin sample Figure 4.19.

The sample B which was used in the UTDR measurements and pressurized through 0 to 5 bars was fully dried and analyzed with the SEM. SEM cross-section image of the layer structure is shown in Figure 4.21.

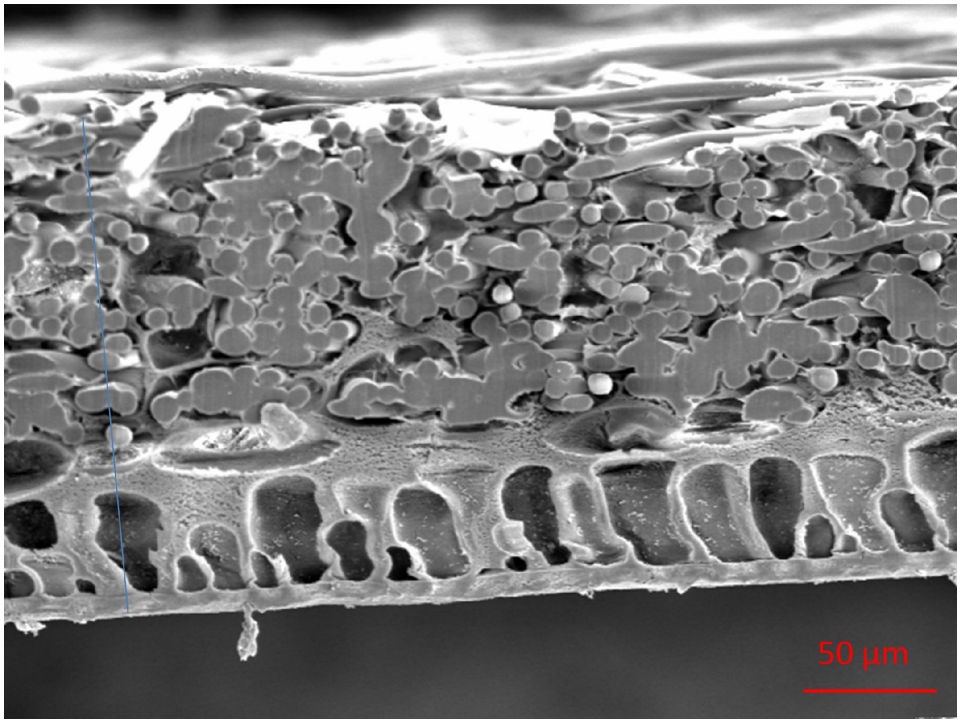

Figure 4.21: SEM cross-section image of the layers structure of the UC030T membrane sample B pressurized through 0 to 5 bar in UTDR measurement.

Total thickness of the compacted membrane is 188 µm the thickness of the porous intermediate layer is 56 µm and support layer 132 µm. Also in figure 4.21 the structure of the porous intermediate layer seems damaged compared to virgin sample.

Also SEM analysis confirms that the compaction has happened and it can be seen on the images that compaction occurs in the porous intermediate layer. Since the membrane material is heterogeneous any exact value of compaction can not be made but the results back up the other methods used in previous sections.

4.7.1 **Discussion**

A scanning electron microscope (SEM) was used to analyze the layer structure of the membranes after the ultrasound measurements. The objective was to find out what happens in the layer structure when compaction occurs. Also SEM analysis confirms that the compaction has happened and it can be seen on the SEM images Figure 4.20

and Figure 4.21 that compaction occurs in the porous intermediate layer. Since the membrane material is heterogeneous any exact value of compaction can not be made but the results back up the other methods used in previous sections.

5 Conclusions

This doctoral thesis focuses on online compaction measurements of the UC030T membranes used in the ultrafiltration applications. A measurement utilizing ultrasound time domain reflectometry was developed for filter equipment operating in the dead-end mode. The system was used to monitor membrane conditions online without affecting the filtering process. Transducers were developed for ultrasound measurements, and a reference transducer was used successfully to improve the resolution of the measurement. According the measurements presented in Chapter 4.1.1 and 4.1.2 it is distinctive that the reference transducer is needed to accurately measure distances in filters where both the pressure and temperature change.

The main contribution of the thesis is the successful introduction of the reference transducer. The accuracy achieved using the reference transducer was less than one micron, which is factor of ten better than reported before. With the help of the transducer, 13 µm membrane compaction was measured in the pressure of 5 bar. The results were confirmed with a permeate flux decline indicating that compaction had taken place. The compaction measurements with a micrometer showed compaction of 23–26 µm. The results are in the same range and confirm the compaction.

Mechanical compaction measurements using a hydraulic piston were made and the result was the same 13 µm as obtained by applying the UTDR. A scanning electron microscope (SEM) was used to study the structure of the samples before and after the compaction. The results are described in more detail in Chapter 4. An overview of the results is shown in Table 5.1.

Table 5.1: Overview of the compaction values using different measurements. Values in micrometers

	UTDR	Flux decline	micrometer	piston	SEM
sample A	13	yes	23	-	yes
sample B	13	yes	26	-	yes
samples C				13	

5.1 Objectives for the future research

Not all questions were answered in the study; hence for the future research, a new filter module is under construction. The type of the filter is one step closer to the filters used in the industry. It is a cross flow filter where the fluid flows on the surface of the membrane. The material is steel to make the changes smaller in the filter module when a higher pressure is applied. The maximum pressure will be above 12 bars.

Also the development of the transducers continues. To achieve higher frequencies meaning a better resolution, piezoceramics have to be reconsidered; a substitute material could be polyvinylidene fluoride (PVDF), which was already studied at the beginning of the research. The poling of the material has to be carried out or alternatively a material that has been polarized has to be used. The matching layer on the surface of the piezomaterial has to be tested to increase the intensity transmitted into water or the fluid used. This is important because the amplitude of the reflection depends on the amplitude transmitted. The reflection amplitude on the fouling layer may be small.

As the developed measurement method can also be applied to monitor the fouling of the membrane, these results are an interesting future research topic. The pump in the current system is not suited for fluids containing solids. Therefore the new system should be designed to do these fouling experiments. The measurements with fouling should be carried out with a process where the fouling layers are in the region of the resolution of the system.

To make longer measurements and to minimize the human error, controlling of the measurement equipment with Labview could be the answer. This would also make the data analysis more automatic.

References

Aerts P., Greenberg A.R., Leysen R., Krantz W.B., Reinsch V.E., Jacobs P.A. (2001), The influence of filler concentration on the compaction and filtration properties of Zirfon®-composite ultrafiltration membranes. *Separation and Purification Technology* Vol. 22–23 pp. 663–669.

Belogol'skii V.A., Sekoyan S.S., Samorukova L.M., Stefanov S.R. and Levtsov V.I. (1999), Pressure dependence of the sound velocity in distilled water, *Measurement Techniques*, Vol. 42, No 4, pp 406–413.

Bilaniuk N. and Wong G. S. K. (1993), Speed of sound in pure water as a function of temperature, *J. Acoust. Soc. Am.* 93(3) pp 1609–1612, as amended by N. Bilaniuk and G. S. K. Wong (1996), Erratum: Speed of sound in pure water as a function of temperature [*J. Acoust. Soc. Am*. 93, 1609–1612 (1993)], J. Acoust. Soc. Am. 99(5), p 3257.

Chen Jim C., Li Qilin, Elimelech Menachem (2004), In situ monitoring techniques for concentration polarization and fouling phenomena in membrane filtration, *Advances in Colloid and Interface Science* Vol. 107 pp. 83–108.

Chen V., Li H., Fane A.G. (2004), Non-invasive observation of synthetic membrane processes – a review of methods. *Journal of Membrane Science*. Vol. 240 pp. 23-44.

Ferroperm catalogue (2010), Available at http://www.ferroperm-piezo.com/, [Accessed on October 2010].

Floyd Thomas L. (2002), *Electronic devices sixth edition*. Prentice Hall International, Inc. ISBN: 0–13–094443–2, pp. 791-792.

Kallioinen M., Pekkarinen M., Mänttäri M., Nuortila-Jokinen J., Nyström M. (1/2007), Comparison of the performance of two different regenerated cellulose ultrafiltration membranes at high filtration pressure. *Journal of Membrane Science* Vol. 294 pp. 93–102.

Kallioinen M. (2/2007), *Regenerated cellulose ultrafiltration membranes in the treatment of pulp and paper mill process waters*, Doctoral Diss., Lappeenranta University of Technology, Lappeenranta, Finland, Acta Universitatis Lappeenrantaensis 307.

Li Jianxin, Sanderson R.D., Jacobs E.P. (1/2002), Non-invasive visualization of the fouling of microfiltration membranes by ultrasonic time-domain reflectometry, *Journal of Membrane Science* Vol. 201 pp. 17–29.

Li Jianxin, Sanderson R.D., Hallbauer D.K., Hallbauer-Zadorozhnaya V.Y. (2/2002), Measurement and modelling of organic fouling deposition in ultrafiltration by ultrasonic transfer signals and reflections. *Desalination* Vol. 146 pp. 177-l85.

Li Jianxin, Hallbauer-Zadorozhnaya V. Yu, Hallbauer D. K., and Sanderson R. D. (3/2002), Cake-layer deposition, growth, and compressibility during microfiltration measured and modeled using a noninvasive ultrasonic technique. *Ind. Eng. Chem. Res.* Vol. 41 pp. 4106-4115.

Li Jianxin, Sanderson R.D. (4/2002), In situ measurement of particle deposition and its removal in microfiltration by ultrasonic time-domain reflectometry, *Desalination* Vol. 146 pp. 169-175.

Li Jianxin, Hallbauer D.K., Sanderson R.D. (2003), Direct monitoring of membrane fouling and cleaning during ultrafiltration using a non-invasive ultrasonic technique. *Journal of Membrane Science* Vol. 215 pp. 33–52

Li Jianxin, Sanderson R.D, Chai G.Y. (2006), A focused ultrasonic sensor for in situ detection of protein fouling on tubular ultrafiltration membranes. *Sensors and Actuators B* Vol. 114 pp. 182–191.

Mairal A. P., Greenberg A. R., Krantz W. B., Bond L. J. (1999), Real-time measurement of inorganic fouling of RO desalination membranes using ultrasonic time-domain reflectometry. *Journal of Membrane Science*. Vol. 159 pp. 185-196.

Mairal A. P., Greenberg A. R., Krantz W. B.(2000), Investigation of membrane fouling and cleaning using ultrasonic time-domain reflectometry, *Desalination* Vol. 130 pp. 45–60.

Peterson R.A., Greenberg A.R., Bond L.J., Krantz W.B. (1998), Use of ultrasonic TDR for real-time noninvasive measurement of compressive strain during membrane compaction. *Desalination* Vol. 116 pp. 115-122.

Reinsch V. E., Greenberg A. R., Kelley S. S., Peterson R., Bond L. J. (2000), A new technique for the simultaneous, real-time measurement of membrane compaction and performance during exposure to high-pressure gas. *Journal of Membrane Science*. Vol. 171 pp. 217–228.

Shull, P.J. (2002), *Nondestructive Evaluation Theory, Techniques, and Applications.* CRC Press Print ISBN: 978-0-8247-8872-8, eBook ISBN: 978-0-203-91106-8, pp. 32–34.

Wika (2010), Pressure gauge scale ranges. Scale spacing and scale numbering per EN 837. Available at http://en-co.wika.de/upload/DS_IN0002_GB_1372.pdf; [Accessed on October 2010].

Xu X., Li J., Li H., Cai Y., Cao Y., He B., Zhang Y. (1/2009), Non-invasive monitoring of fouling in hollow fiber membrane via UTDR, *Journal of Membrane Science*, Vol. 326 pp. 103–110.

Xu Xincheng, Li Jianxin, Xu Nini, Hou Yanlin, Lin Jiebin (2/2009), Visualization of fouling and diffusion behaviors during hollow fiber microfiltration of oily wastewater by ultrasonic reflectometry and wavelet analysis, *Journal of Membrane Science* Vol. 341 pp. 195–202.

Appendix A: Additional tables

Coefficients for the Belogol'skii equations (2.2–2.6)

a_{00}	1402.38744
a_{10}	5.03836171
a_{20}	$-5.81172916 \times 10^{-2}$
a_{30}	$3.34638117 \times 10^{-4}$
a_{40}	$-1.48259672 \times 10^{-6}$
a_{50}	$3.16585020 \times 10^{-9}$
a_{01}	1.49043589
a_{11}	$1.077850609 \times 10^{-2}$
a_{21}	$-2.232794656 \times 10^{-4}$
a_{31}	$2.718246452 \times 10^{-6}$
a_{02}	$4.31532833 \times 10^{-3}$
a_{12}	$-2.938590293 \times 10^{-4}$
a_{22}	$6.822485943 \times 10^{-6}$
a_{32}	$-6.674551162 \times 10^{-8}$
a_{03}	$-1.852993525 \times 10^{-5}$
a_{13}	$1.481844713 \times 10^{-6}$
a_{23}	$-3.940994021 \times 10^{-8}$
a_{33}	$3.939902307 \times 10^{-10}$

Appendix A: Additional tables

Temperatures in pressures through 1–5 bar in the measurement of accuracy.

Time	T@1 bar	T@2 bar	T@3 bar	T@4 bar	T@5 bar
1	24.6	25.7	25.6	26	26.7
2	24.8	25.6	25.7	25.9	26.5
3	25	25.8	25.6	26.2	26.4
4	25.2	25.9	25.9	26.5	26.5
5	25.3	25.8	25.9	26.3	26.6
6	25.3	25.7	25.7	25.9	26.5
7	25.3	25.6	25.6	26.4	26.3

Appendix B: Membrane UC030T Sample A measurement table

Membrane compaction UC030T SampleA

1 bar					
Clock	**Time(µs)**	**Time(µs)**	**T(°C)**	**T(°C)**	**flux**
	membrane	ref.	filter	tank	g/min
9:45	78,3635	69,9793	22,8	22,3	17,8
9:55	78,3122	69,9317	23,2	22,7	18,2
10:05	78,2649	69,8944	23,6	23	18,2
10:15	78,2378	69,864	23,9	23,3	18,4
10:25	78,2018	69,8305	24,1	23,6	18,4
10:35	78,1881	69,818	24,2	23,7	18,4
10:45	78,1562	69,789	24,5	24	18,4

1 bar					
Clock	**Time(µs)**	**Time(µs)**	**T(°C)**	**T(°C)**	**flux**
	membrane	ref.	filter	tank	g/min
10:50	78,1428	69,777	24,6	24	18,5
11:00	78,111	69,7479	24,8	24,2	18,6
11:10	78,0874	69,7234	25	24,3	18,6
11:20	78,0699	69,7099	25,2	24,4	18,4
11:30	78,0598	69,6983	25,3	24,7	18,6
11:40	78,0605	69,6982	25,3	24,6	18,8
11:50	78,0405	69,6835	25,3	24,8	18,8

2 bar					
Clock	**Time(µs)**	**Time(µs)**	**T(°C)**	**T(°C)**	**flux**
	membrane	ref.	filter	tank	g/min
11:55	78,265	69,6426	25,7	24,8	34,9
12:05	78,2768	69,6471	25,6	24,8	34
12:15	78,2508	69,623	25,8	24,9	34
12:25	78,2514	69,6209	25,9	24,9	34
12:35	78,2658	69,6302	25,8	24,9	34
12:45	78,2682	69,631	25,7	24,9	33,6
12:55	78,285	69,6451	25,6	24,9	33,5

Appendix B: Membrane UC030T Sample A measurement table

3 bar					
Clock	**Time(µs)**	**Time(µs)**	**T(°C)**	**T(°C)**	**flux**
	membrane	ref.	filter	tank	g/min
13:03	78,4052	69,6398	25,6	24,6	47,6
13:10	78,4043	69,6323	25,7	24,7	47,2
13:20	78,4113	69,6342	25,6	24,6	48,8
13:30	78,37	69,5966	25,9	25	49,2
13:40	78,3763	69,6008	25,9	25	48,7
13:50	78,4144	69,6309	25,7	24,8	49,2
14:00	78,4153	69,6303	25,6	24,8	48,2

4 bar					
Clock	**Time(µs)**	**Time(µs)**	**T(°C)**	**T(°C)**	**flux**
	membrane	ref.	filter	tank	g/min
14:05	78,4629	69,5804	26	25	64,4
14:15	78,5005	69,6026	25,9	24,7	62,4
14:25	78,4494	69,5536	26,2	25	62,8
14:35	78,4222	69,5293	26,5	25,1	61,6
14:45	78,4536	69,555	26,3	24,8	61,2
14:55	78,5062	69,5994	25,9	24,6	60,2
15:05	78,441	69,541	26,4	25,1	60,8

5 bar					
Clock	**Time(µs)**	**Time(µs)**	**T(°C)**	**T(°C)**	**flux**
	membrane	ref.	filter	tank	g/min
15:10	78,5051	69,4978	26,7	24,9	72,8
15:20	78,5371	69,5156	26,5	24,7	72,3
15:30	78,5711	69,5399	26,4	24,7	71,2
15:40	78,563	69,5267	26,5	24,7	70,6
15:50	78,5478	69,5107	26,6	24,8	70,2
16:00	78,5757	69,5282	26,5	24,8	69,3
16:10	78,598	69,546	26,3	24,8	69

ACTA UNIVERSITATIS LAPPEENRANTAENSIS

365. POLESE, GIOVANNI. The detector control systems for the CMS resistive plate chamber at LHC. 2009. Diss.

366. KALENOVA, DIANA. Color and spectral image assessment using novel quality and fidelity techniques. 2009. Diss.

367. JALKALA, ANNE. Customer reference marketing in a business-to-business context. 2009. Diss.

368. HANNOLA, LEA. Challenges and means for the front end activities of software development. 2009. Diss.

369. PÄTÄRI, SATU. On value creation at an industrial intersection – Bioenergy in the forest and energy sectors. 2009. Diss.

370. HENTTONEN, KAISA. The effects of social networks on work-team effectiveness. 2009. Diss.

371. LASSILA, JUKKA. Strategic development of electricity distribution networks – Concept and methods. 2009. Diss.

372. PAAKKUNAINEN, MAARET. Sampling in chemical analysis. 2009. Diss.

373. LISUNOV, KONSTANTIN. Magnetic and transport properties of II-V diluted magnetic semiconductors doped with manganese and nickel. 2009. Diss.

374. JUSSILA, HANNE. Concentrated winding multiphase permanent magnet machine design and electromagnetic properties – Case axial flux machine. 2009. Diss.

375. AUVINEN, HARRI. Inversion and assimilation methods with applications in geophysical remote sensing. 2009. Diss.

376. KINDSIGO, MERIT. Wet oxidation of recalcitrant lignin waters: Experimental and kinetic studies. 2009. Diss.

377. PESSI, PEKKA. Novel robot solutions for carrying out field joint welding and machining in the assembly of the vacuum vessel of ITER. 2009. Diss.

378. STRÖM, JUHA-PEKKA. Active*du*/d*t* filtering for variable-speed AC drives. 2009. Diss.

379. NURMI, SIMO A. Computational and experimental investigation of the grooved roll in paper machine environment. 2009. Diss.

380. HÄKKINEN, ANTTI. The influence of crystallization conditions on the filtration characteristics of sulphathiazole suspensions. 2009. Diss.

381. SYRJÄ, PASI. Pienten osakeyhtiöiden verosuunnittelu – empiirinen tutkimus. 2010. Diss.

382. KERKKÄNEN, ANNASTIINA. Improving demand forecasting practices in the industrial context. 2010. Diss.

383. TAHVANAINEN, KAISA. Managing regulatory risks when outsourcing network-related services in the electricity distribution sector. 2010. Diss.

384. RITALA, PAAVO. Coopetitive advantage – How firms create and appropriate value by collaborating with their competitors. 2010. Diss.

385. RAUVANTO, IRINA. The intrinsic mechanisms of softwood fiber damage in brown stock fiber line unit operations. 2010. Diss.

386. NAUMANEN, VILLE. Multilevel converter modulation: implementation and analysis. 2010. Diss.

387. IKÄVALKO, MARKKU. Contextuality in SME ownership – Studies on owner-managers´ ownership behavior. 2010. Diss.

388. SALOJÄRVI, HANNA. Customer knowledge processing in key account management. 2010. Diss.

389. ITKONEN, TONI. Parallel-operating three-phase voltage source inverters – Circulating current modeling, analysis and mitigation. 2010. Diss.

390. EEROLA, TUOMAS. Computational visual quality of digitally printed images. 2010. Diss.

391. TIAINEN, RISTO. Utilization of a time domain simulator in the technical and economic analysis of a wind turbine electric drive train. 2010. Diss.

392. GRÖNMAN AKI. Numerical modelling of small supersonic axial flow turbines. 2010. Diss.

393. KÄHKÖNEN, ANNI-KAISA. The role of power relations in strategic supply management – A value net approach. 2010. Diss.

394. VIROLAINEN, ILKKA. Johdon coaching: Rajanvetoja, taustateorioita ja prosesseja. 2010. Diss.

395. HONG, JIANZHONG. Cultural aspects of university-industry knowledge interaction. 2010. Diss.

396. AARNIOVUORI, LASSI. Induction motor drive energy efficiency – Simulation and analysis. 2010. Diss.

397. SALMINEN, KRISTIAN. The effects of some furnish and paper structure related factors on wet web tensile and relaxation characteristics. 2010. Diss.

398. WANDERA, CATHERINE. Performance of high power fiber laser cutting of thick-section steel and medium-section aluminium. 2010. Diss.

399. ALATALO, HANNU. Supersaturation-controlled crystallization. 2010. Diss.

400. RUNGI, MAIT. Management of interdependency in project portfolio management. 2010. Diss.

401. PITKÄNEN, HEIKKI. First principles modeling of metallic alloys and alloy surfaces. 2010. Diss.

402. VAHTERISTO, KARI. Kinetic modeling of mechanisms of industrially important organic reactions in gas and liquid phase. 2010. Diss.

403. LAAKKONEN, TOMMI. Distributed control architecture of power electronics building-block-based frequency converters. 2010. Diss.

404. PELTONIEMI, PASI. Phase voltage control and filtering in a converter-fed single-phase customer-end system of the LVDC distribution network. 2010. Diss.

405. TANSKANEN, ANNA. Analysis of electricity distribution network operation business models and capitalization of control room functions with DMS. 2010. Diss

406. PIIRAINEN, KALLE A. IDEAS for strategic technology management: Design of an electronically mediated scenario process. 2010. Diss.

407. JOKINEN, MARKKU. Centralized motion control of a linear tooth belt drive: Analysis of the performance and limitations. 2010. Diss.

408. KÄMÄRI, VESA. Kumppanuusohjelman strateginen johtaminen – Monitapaustutkimus puolustushallinnossa. 2010. Diss.